

DESIGN OF A CABLE-STAYED PRECAST POST-TENSIONED BOX GIRDER BRIDGE

by

Bernard Joseph Deneke

Thesis submitted to the Faculty of the
Virginia Polytechnic Institute and State University
in partial fulfillment of the requirements for the degree of
Master of Science in Civil Engineering

APPROVED:

R.M. Barker, Chairman

S.M. Holzer

D.A. Garst

December, 1986

Blacksburg, Virginia

DESIGN OF A CABLE-STAYED PRECAST POST-TENSIONED BOX GIRDER BRIDGE

by

Bernard Joseph Deneke

R.M. Barker, Chairman

(ABSTRACT)

An overview of current practice in the field of cable-stayed post-tensioned precast box girder technology and construction is presented. Likewise, a preliminary design for a 600 foot main span cable-stayed post-tensioned box girder bridge is presented. The analysis considers dead load, and live loadings acting on the girder using nonlinear analysis assumptions governing the bridges response.

Since specific codes governing cable-stayed bridges are not presented in the AASHTO Code, analysis was based on allowable stresses where requirements in the AASHTO code were not specified.

Acknowledgements

I would like to thank my parents for their support and encouragement which they have given me throughout my years of schooling. Without them, it would not have been possible.

Special thanks to Dr. R.M. Barker for serving as my Committee Chairman and providing me with guidance and support. Special thanks is also extended to Dr. S.M. Holzer for serving on my committee and allowing me to use ABAQUS for the analysis required in the design of the bridge. Likewise, special thanks to Professor D.A. Garst for providing me with manufacturer's cable data and serving on my committee.

Table of Contents

PURPOSE AND SCOPE	1
CHAPTER 1	2
HISTORY OF CABLE-STAYED BRIDGES AND CURRENT TECHNOLOGY	2
1.1 HISTORY OF CABLE-STAYED BRIDGES.	2
1.2 CURRENT TECHNOLOGY	4
1.2.1 NONLINEAR BEHAVIOR OF CABLE-STAYED BRIDGES	5
1.2.2 CABLE THEORY ASSOCIATED WITH CABLE-STAYED BRIDGES	6
1.3 CONSTRUCTION OF CONCRETE SEGMENTAL CABLE-STAYED BRIDGES	11
CHAPTER 2	14
COMPONENTS OF CONCRETE SEGMENTAL CABLE-STAYED BRIDGES	14
2.1 SEGMENTS FORMING THE GIRDER	14
2.2 SEGMENT JOINTS	17
2.3 DIAPHRAGMS	17
2.4 TOWER CONFIGURATIONS	18
2.5 CABLE ARRANGEMENT	18
2.6 CABLES AND ANCHORAGE SYSTEMS	21
2.7 POST-TENSIONING	23
CHAPTER 3	24
A PRELIMINARY DESIGN OF A 600 FOOT MAIN SPAN CABLE-STAYED BRIDGE	24
3.1 SITE CHARACTERISTICS	24
3.2 ASSUMPTIONS MADE FOR THE PRELIMINARY DESIGN	26
3.3 PRELIMINARY SIZE OF PRECAST SEGMENT CROSS SECTION	29

3.4 TRANSVERSE ANALYSIS OF THE BOX SECTION	32
3.4 MAIN TOWER AND CABLE-STAY DESIGN	44
3.5 DEVELOPMENT OF LONGITUDINAL SHEAR AND MOMENT ENVELOPES	48
3.6 PRESTRESSING DESIGN OF THE GIRDER FOR THE COMPLETED STRUC- TURE	56
CHAPTER 4	64
CONCLUSION	64
REFERENCES	66
VITA	67

PURPOSE AND SCOPE

The purpose of this thesis is to provide the reader with a summarized literature review of existing theories to date in the advanced form of bridge design known as: cable-stayed bridges. The components of these types of bridges as well as present design concepts are also presented. Likewise, a design of a 600 foot main span cable-stayed bridge is presented using theories stated by authors in the fields of segmental box girder bridges and cable-stayed bridges. Reference is made to AASHTO where specifications can be considered.

CHAPTER 1

HISTORY OF CABLE-STAYED BRIDGES AND CURRENT TECHNOLOGY

1.1 HISTORY OF CABLE-STAYED BRIDGES.

The stayed bridge concept has been shown to exist as early as the seventeenth-century. The use of stays was conceived as a way of reducing pier supports. However, this concept was not readily acceptable because of early failures that occurred. The first stayed bridge design was credited to C.J. Loscher in 1784. His design incorporated the use of wooden stays attached to a wooden bridge deck. The first bridge to incorporate the use of cables as stays was the Kings Meadow Foot Bridge built in 1817 whose design is credited to Redpath and Brown, two engineers from Britain.

Early failures of stayed bridges hindered their acceptance. The earliest recorded collapse of a stayed-bridge occurred in 1818 when wind oscillation caused stay-chains to break on a pedestrian bridge crossing the Tweed River near Dryburg-Abby England. A second failure occurred in 1824 when a 256 foot span on the Saale river near Nienburg, Germany collapsed. Although the cause of the failure is not known, it was thought to be due to overloading. On early bridge designs, cables or chains which comprised the stays were attached with considerable amounts of sag in them when they were under the influence of only dead load. Once the live load was placed on them they underwent considerable displacements. These displacements were believed to overstress the girder. Furthermore, these failures were attributed to insufficient technology and knowledge of material properties. Discussion of these failures among engineers during this time, prompted engineers to rely on other concepts in bridge design. For long span bridges, the suspension bridge was used. John Roebling, an engineer and a manufacturer of steel cables, still insisted on the incorporation of

cable-stays but in conjunction with the suspension cables. The stays were considered as being comforting safety features and were later omitted in suspension designs.

The rebirth of the cable-stayed bridge occurred in Europe in the 1950's. Three bridges spanning the Rhine River which were damaged during World War II were replaced with cable-stayed bridges. These bridges were simple in form and fabricated from steel. The first cable-stayed bridge to incorporate a concrete deck was the Tempul Aqueduct crossing the Guadalete River in Spain. The stays were incorporated to compensate for two piers which were too difficult to construct due to adverse terrain features. On July 5, 1957 the first concrete cable-stayed bridge was opened to traffic in the United States spanning the Yakima River in Benton City, Washington. To date, several cable-stayed bridges have been constructed or are in the design stages in the span range from 1000 - 1200 feet. Likewise, shorter span ranges of 500 - 700 feet have been shown to be economical and designs are presently being considered.

In a study conducted by Leonhardt and Zellner (11), cable-stayed bridges were shown to possess an inherent advantage over suspension bridges in the long span ranges. On suspension bridges, unsymmetrical live load patterns cause considerably larger deflections as opposed to deflections on a cable-stayed bridge of similar proportions. However, dead load deflection of the suspension bridge is 77% of that of a cable-stayed bridge. The live load deflection characteristics can be explained by investigating the load paths taken by a vertical load acting on the bridge deck. In the cable-stayed system, the vertical load is taken by the cables and transferred directly to the tower which undergoes minimal deflections. On the other hand, in the suspension system the vertical load is transferred to the main catenary cable which seeks a new equilibrium configuration. This accounts for the large live load deflections associated with suspension bridges in comparison with the cable-stayed bridge. In the study, Leonhardt projected that with proper aerodynamic streamlining a cable-stayed bridge with a span of up to 2300 feet can be achieved. Thus, the cable-stayed bridge may become competitive with the suspension bridge in the exceptionally long span ranges. Other advantages of a concrete cable-stayed bridge are:

- Span-to-girder depth ratios can vary from 45 to 100 in accordance with proper aerodynamic streamlining, thus, giving them a streamline appearance.
- Concrete used as a structural material provides good damping characteristics and is less susceptible to aerodynamic vibrations.
- Horizontal cable-stay forces cause compressive stresses which are ideal for concrete structures. Likewise, they counteract bending stresses.
- Steel area of cable-stays is comparatively small. Thus, providing good material utilization.
- Live load deflections are small in comparison with dead load deflections.
- Erection of the superstructure is easily achieved with current technology.

1.2 CURRENT TECHNOLOGY

Cable-stayed bridges are statically indeterminate systems to a large degree and are very difficult to analyze. These systems may be comprised of beam elements and or truss elements in conjunction with cable elements. The cable element alone presents many of the difficulties associated with the nonlinear analysis of cable-stayed bridges. To perform a detailed analysis of a cable-stayed bridge, programs specifically designed to incorporate the elements mentioned to form the model must be developed. Finite element programs to model areas of high stress concentrations such as at pier, tower, and girder connections and at cable anchorages should be used to determine critical stress locations in these areas. Presently, there exist no design aids in AASHTO (1) to simplify design requirements for cable-stayed bridges. Where specifications in AASHTO may apply, such as loads, they must be satisfied. Companies which are reluctant to venture into the design of cable-stayed

bridges must provide detailed analysis procedures and calculations for consent by the governing board considering the design (AASHTO or FHWA). One area of concern is in the area of flexibility. AASHTO limits the live load deflection to $1/800$ of the span. Deflections of current cable-stayed bridges have shown deflections considerably greater than this (Severn Bridge at Cologne $1/225$ the span). Stress limitations on high strength cables which comprise the cable-stays are not specifically outlined in AASHTO. Many engineers look to the German Code, DIN 4114 (14), or AISI Code for Building Safety (14) for allowable stress ranges. When AASHTO adopts code requirements governing the design of cable-stayed bridges there will be a gradual trend to accept cable-stayed bridges as a practical concept. Economically, it will allow more engineers to consider it as a design alternative.

1.2.1 NONLINEAR BEHAVIOR OF CABLE-STAYED BRIDGES

Cable-stayed bridges exhibit nonlinear elastic behavior due to large displacements, bending moment-axial force interaction, and catenary action of cables. Since the girder and tower elements which comprise the bridge are slender and carry high compressive forces and bending moments, nonlinear analysis should be carried out in the design. There are two theories that engineers base assumptions on how the nonlinear analysis should be carried out. The first of these follows the German Code, DIN 4114, which states that the nonlinear analysis should be carried out with a loading of $1.75(\text{DEAD LOAD} + \text{LIVE LOAD})$ or $1.5(\text{DL} + \text{LL} + \text{W} + \text{T} + \dots)$ and at no time shall the material yield stress be exceeded (14). The second, as stated by Podolny (11), assumes that the nonlinear behavior is only associated with the dead load and for live loading the analysis should be carried out using linear theory. He attributes this to the stiffening of the cables as they become taut under the dead load.

In view of both theories, the German Code provides conservative results and is impractical for very long spans and the assumption by Podolny requires considerable engineering judgement

which is influenced by structural stiffness considerations and dead load to live load ratios. Comparisons between linear and nonlinear analysis have shown that stresses at critical sections are approximately 12% greater using nonlinear analysis as opposed to those using linear analysis (5).

1.2.2 CABLE THEORY ASSOCIATED WITH CABLE-STAYED BRIDGES

In the analysis of a cable-stayed bridge the force exerted by a cable is assumed to act along an inclined chord. Thus, the cable element is assumed to be a straight member. Changes in sag and stiffness are accounted for by varying the modulus of elasticity of the straight element which models the cable. Several authors have investigated this theory and through the use of the catenary equations shown below (Eqs. 1.1-1.5), they have adopted the equation presented by the German engineer, J.H. Ernst (11), known as Ernst's equation (Eq. 1.6).

$$H = \frac{wL^2}{8f'} \quad (1.1)$$

$$T_{\max} = H [1 + (\tan \theta + 4\eta)^2]^{1/2} \quad (1.2)$$

$$V_T = H \tan \theta + \frac{wL}{2} \quad (1.3)$$

$$S \cong L \sec \theta \left[1 + \frac{8\eta^2}{3 \sec^4 \theta} \right] \quad (1.4)$$

$$\Delta S_s \cong \frac{HL}{A_{\text{cable}} E_{\text{act}}} \sec \theta \left[1 + \frac{16\eta^2}{3 \sec^4 \theta} \right] \quad (1.5)$$

$$E_{\text{eq}} = \frac{E_{\text{act}}}{1 + \frac{(\gamma L)^2}{12\sigma^3} E_{\text{act}}} \quad (1.6)$$

where (in reference to Fig. 1):

- H = Horizontal component of cable force
- w = Uniform load per unit length of horizontal projection
- L = Span
- f' = Cable sag
- T_{\max} = Maximum tension force
- $\eta = f'/L$, Sag ratio
- V_T = Vertical component of cable force at top
- V_B = Vertical component of cable force at bottom
- S = Cable length
- ΔS_s = Cable elongation due to cable tension stress
- E_{act} = Actual modulus of elasticity of cable
- E_{eq} = Equivalent modulus of elasticity
- γ = Specific weight of cable
- σ_{\max} = Cable tension stress
- A_{cable} = Steel area of cable

The stress in the cable can be determined from catenary equations and can be expressed in the following form (Eq. 1.7):

$$\sigma_{\max} = \frac{\gamma L}{8\eta \cos \theta} [1 + (\tan \theta + 4\eta)^2]^{1/2} \quad (1.7)$$

In reference to Figure 2, the equivalent modulus of elasticity, as defined by Eq. 1.6, approximates the true modulus of elasticity of the cable at approximately 30 percent of the ultimate strength of 200 ksi ($L=300$ feet). Likewise, in Figure 3, the equivalent modulus of elasticity approximates the true one at a sag ratio of $1/300$ ($L=160$ feet). Typical sag ratios of cables associated with cable-stayed bridges are from $1/500$ to $1/700$ under service loads. Thus, the cable responds similar to a truss element if one ignores the end forces produced by its weight.

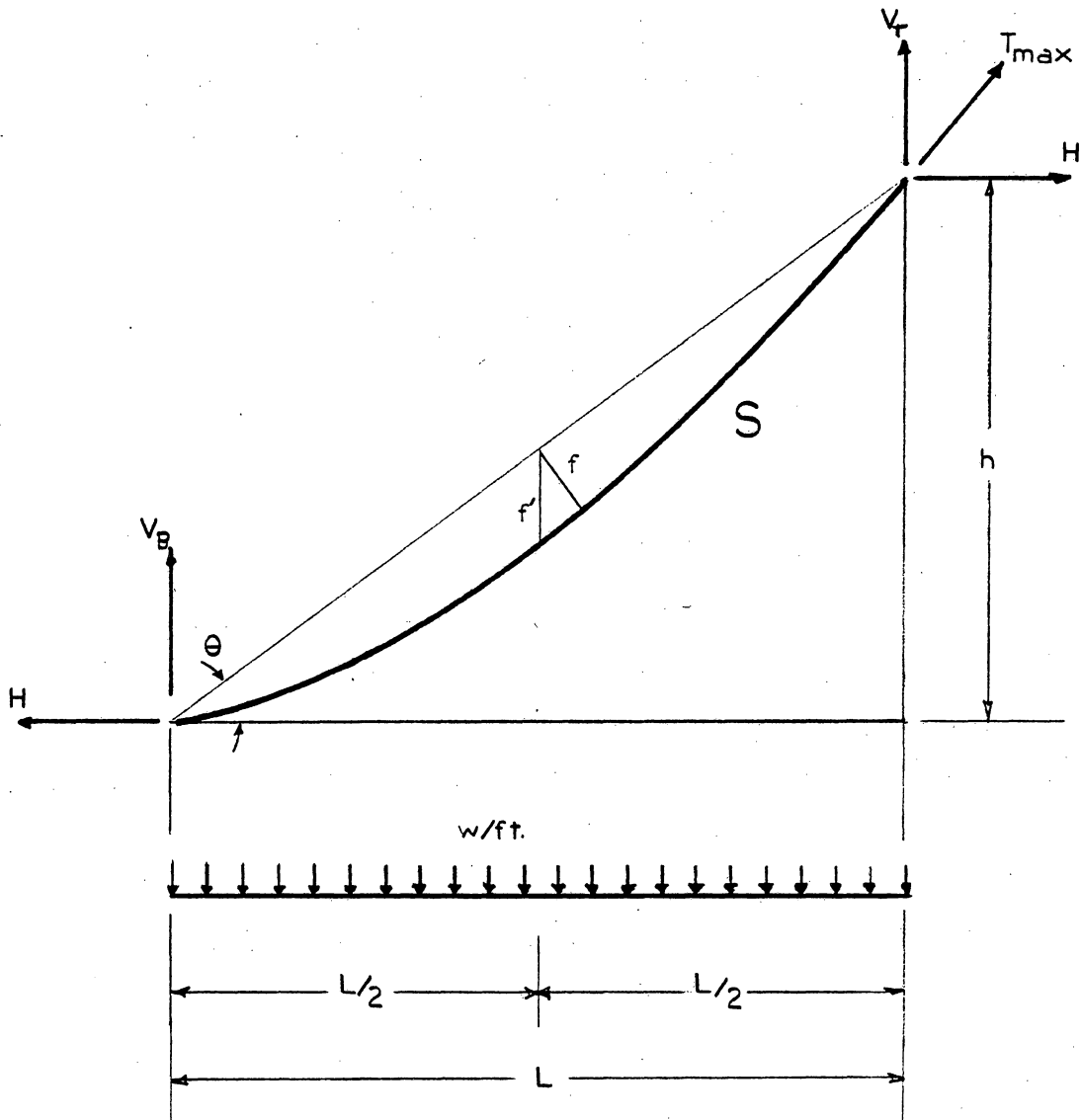


Figure 1. Inclined cable chord.

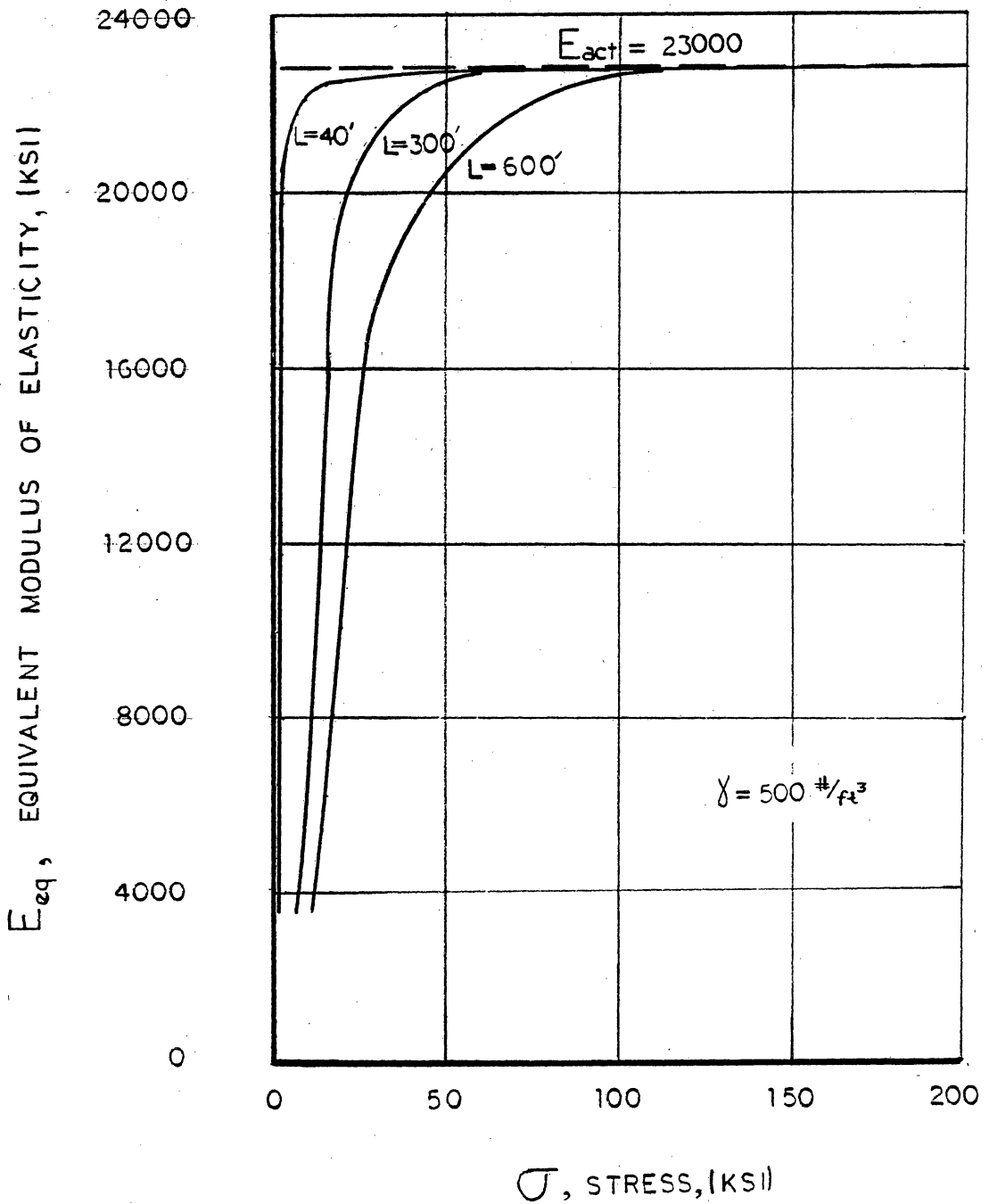


Figure 2. Stress Verses Equivalent Modulus of Elasticity.

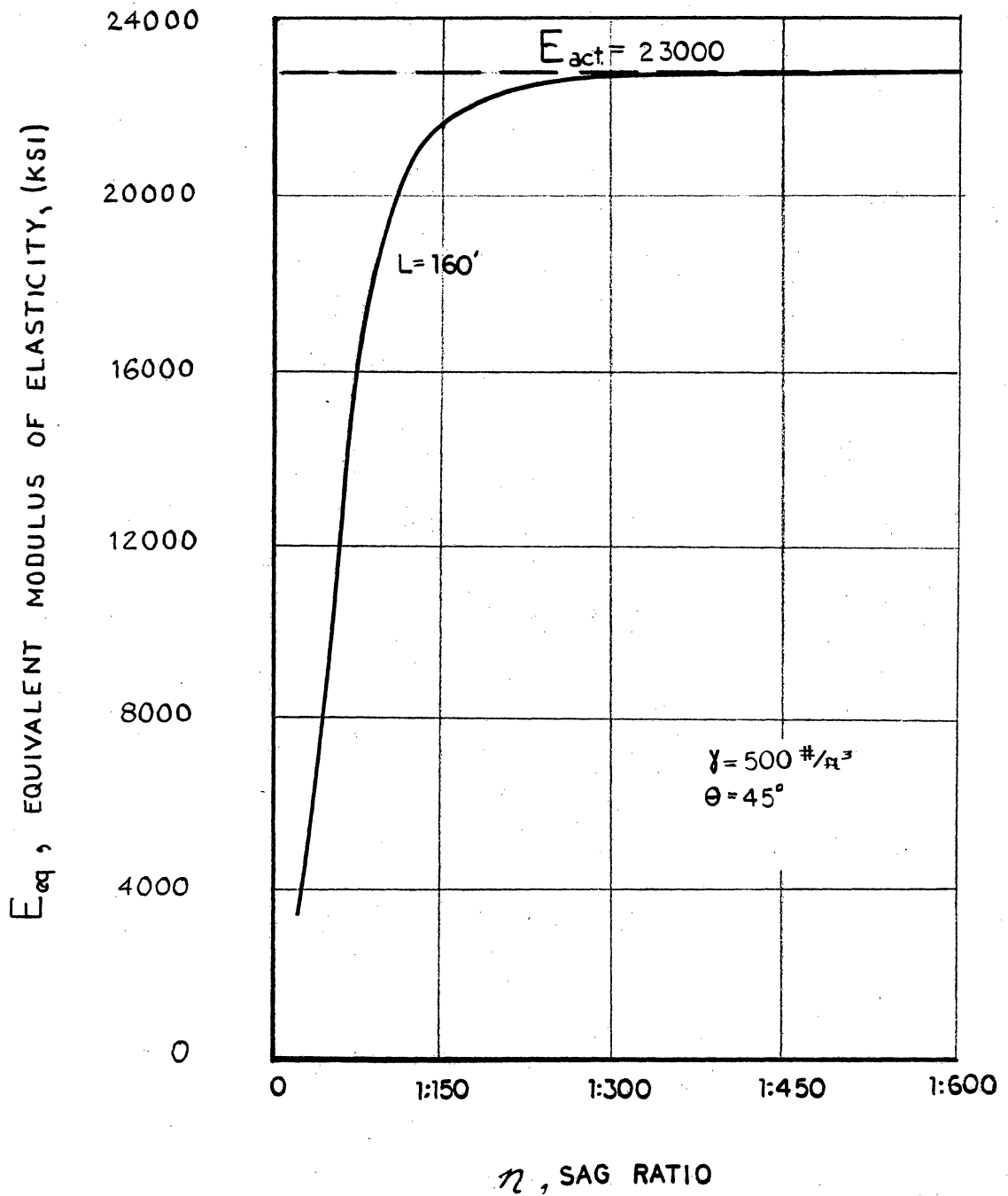


Figure 3. Sag Ratio Verses Equivalent Modulus of Elasticity.

1.3 CONSTRUCTION OF CONCRETE SEGMENTAL CABLE-STAYED BRIDGES

Concrete cable-stayed bridges are typically constructed from precast segments using the balanced cantilever method of construction. Other construction methods provide increasing complexity to an already difficult problem. The use of precast segments allows:

- Superior dimensional tolerances and control of material properties.
- Ease of geometric changes through the use of stationary adjustable forms.
- Greater strength during post-tensioning and cable-stay stressing operations.
- Ease of erection and construction techniques.

Cable attachment of concrete cable-stayed bridges generally occurs on every segment or, more often, every other segment (20 - 35 feet). This allows for adequate stress distribution and reduction in complexity of post-tensioning tendon layout. Cable-stayed bridges not utilizing this procedure of stay attachment require additional methods to control increased cantilever stresses and cable stresses. This usually results in the use of temporary supports.

The balanced cantilever method of construction is utilized when partial fixity can be achieved at the main piers. Generally, this is provided for during construction to increase stability on spans which in the final configuration receive no interaction between the main piers and girder except through the cable-stays. Using the balanced cantilever method of construction, once the main pier and tower have been completed, construction progresses outward in both directions (Fig. 4). The pier and tower can be cast-in-place using slip forms or precast. Both methods of construction require the use of a derrick to be attached to the pier or tower to pour or place segments at great heights. Once the pier and tower have been constructed, segments forming the girder are placed

using a derrick in an alternating sequence on each side of the pier. Segments with cable anchorages are typically attached simultaneously on each side of the pier since the cable passing through the tower is usually continuous. This allows for the cable stressing to proceed in a manner in which they can be fully utilized. Cantilevering continues out from the main pier until the side span reaches the approach span. This sequence is repeated for the other half of the span. The closure segment can be poured-in-place or a precast segment. Thus, the entire span becomes continuous.

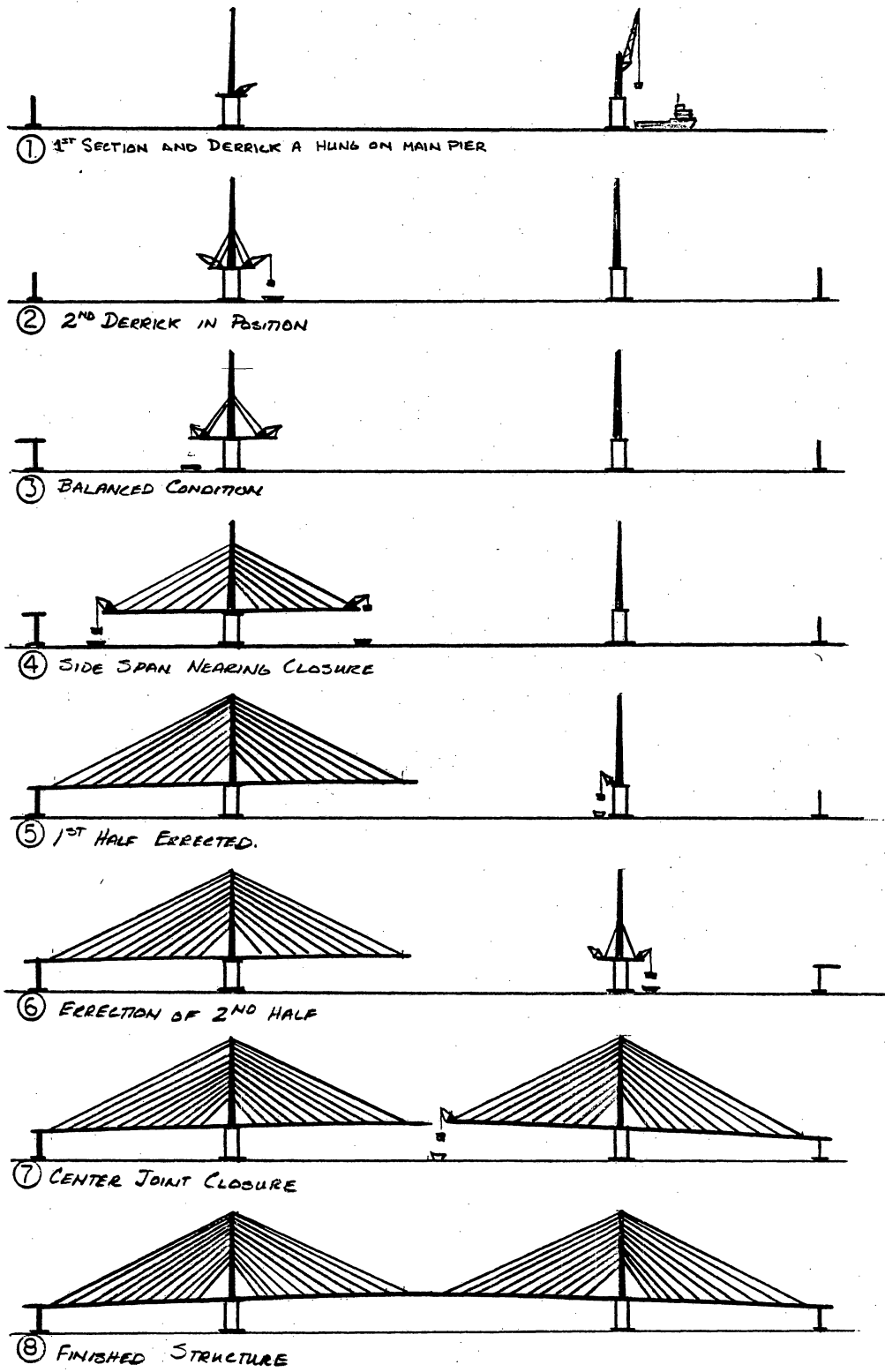


Figure 4. Balanced cantilever construction of a cable-stayed bridge

CHAPTER 2

COMPONENTS OF CONCRETE SEGMENTAL CABLE-STAYED BRIDGES

In this section the various components of making up the segmental cable-stayed bridge are discussed. They include the concrete box girder segments, tower configurations, and cable systems.

2.1 SEGMENTS FORMING THE GIRDER

The box girder is considered to be an efficient section and is commonly used to take advantage of the following properties:

- Material is concentrated at the extreme fibers to carry bending stresses.
- The box shaped section provides good torsional stability for carrying unsymmetrical loads acting transversely along the top flange (12).
- Large flange areas permit full capacity of post tensioning tendons to be utilized without loss in the lever arm under ultimate loads (12).
- The box section provides the least required amount of post tensioning steel for a given amount of concrete.
- Trapezoidal box sections provide good aerodynamic stability.

One measure of the box sections efficiency is given by the following equation (Eq. 2.1) (12).

$$\rho = \frac{r^2}{c_1 c_2} \quad (2.1)$$

where:

- r = Radius of gyration, $\sqrt{I/A}$
- c_1 = Distance from neutral axis to extreme top fiber
- c_2 = Distance from neutral axis to extreme bottom fiber

The typical efficiency of a box girder section is 0.6 as opposed to that of a rectangular section of 0.3.

Single cell girders have a typical width not greater than 40 feet. However, with proper provisions to carry dead and live loads, the width can be increased without the use of an intermediate web. These provisions may include the use of hollow core slabs, incorporation of a bracing scheme (Fig. 5a), or, as recommended by AASHTO, transverse post-tensioning.

Depth of the cross section is dependent on span length, loads, aerodynamic streamlining, and cable arrangement. Current cable-stayed bridges show a depth-to-span ratio of 1:50 to 1:250. A design for the Baytown Bridge over the Houston Ship Channel has a ratio of 1:750.

Segment length is a function of mainly erection considerations. Likewise, cable spacing plays an important role in determining segment length. These are two crucial parameters, since cables on current designs are spaced approximately every 20 to 30 feet. The Pasco-Kennewick bridge has cables spaced every 27 feet attached to every segment. The Sunshine Skyway Bridge has cables spaced every 24 feet with attachments on every other segment.

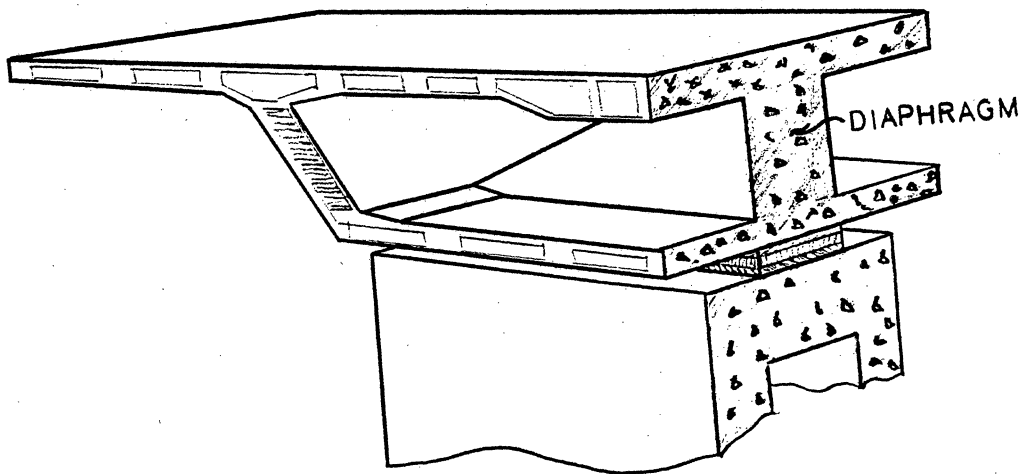
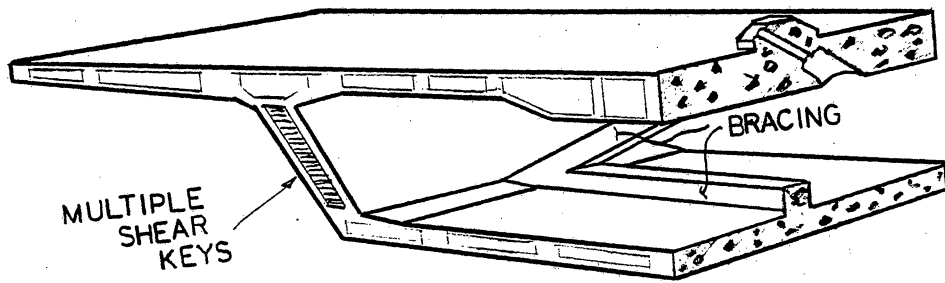


Figure 5. Box section with interior bracing and diaphragm.

2.2 SEGMENT JOINTS

The segment joint is an important detail where force transfer between segments takes place and geometry alignment corrections are made. Shear stresses are transferred at the joint through the use of multiple shear keys (Fig. 5a). This is done to distribute the shear stress across the entire joint, alleviating the shear stress concentration when only one shear key is used as in old designs. Alignment keys are placed in the top and bottom flanges to ensure alignment during the erection stages. These keys help guide the segment into the proper position. Minor adjustments in alignment can be made at the joint face during the erection stages through the use of shims placed in the joint. Although it is not favorable to use the shims, it is presently used to control discrepancies in vertical alignment.

2.3 DIAPHRAGMS

The use of diaphragms located over the supports alleviates the reaction force at the support transferred directly to the bottom flange (Fig. 5b). The use of diaphragms distributes the reaction force over the cross section of the girder. AASHTO states that diaphragms shall be used at the ends of spans and that intermediate diaphragms are not required on straight spans. Another function of the diaphragm is to maintain the geometry of the box while under the influence of transverse loads.

2.4 TOWER CONFIGURATIONS

The towers of cable-stayed bridges must be able to withstand high axial compressive stresses as well as bending stresses. Their configuration can range from simple cantilevers to complex frames for carrying high bending stresses at the base of the tower (Fig. 6a). Each has distinct advantages and disadvantages.

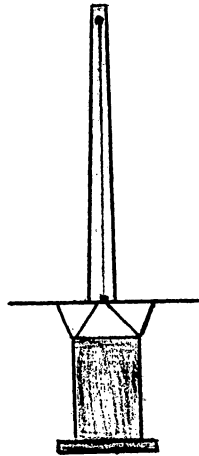
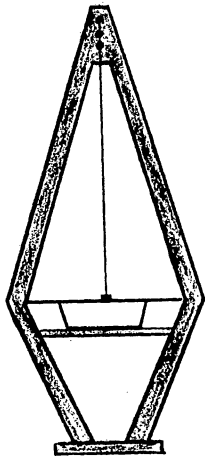
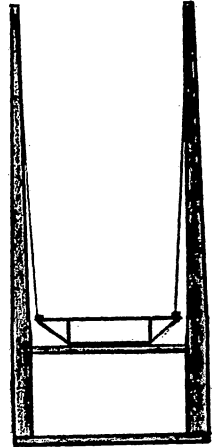
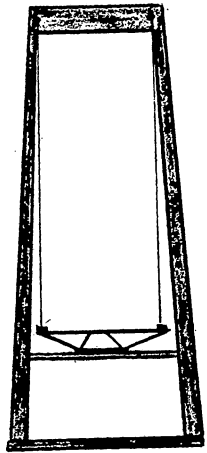
The most common of these is the fixed base cantilever constructed of hollow rectangular sections. Fixity at the base provides for added structural stiffness and readily facilitates the balanced cantilever method of construction. Bending stresses at the base of the tower may present problems, but through the application of prestressing and the presence of axial compression they are generally controllable.

The height of the tower is primarily a function of the span length and cable configuration with some emphasis given to aesthetics.

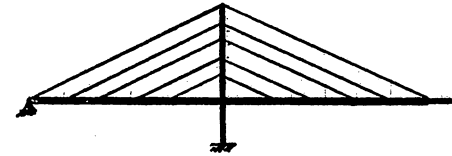
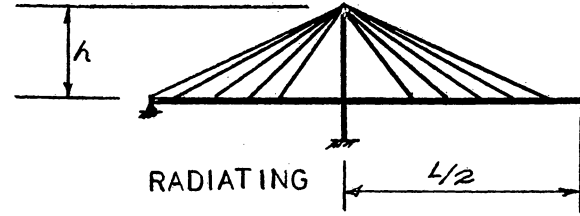
Bending in the tower occurs in both the longitudinal and transverse directions. Longitudinally it is caused primarily by dead and live loads acting on the girder. This can be alleviated by attempting to balance horizontal components of cable forces on each side of the tower. Typically this is done by using cable saddles in the tower or adjusting cable forces during final stressing operations. Transverse bending results from wind loads acting on the structure. In the design for transverse bending, maximum wind velocities at the site are usually used for design considerations. Likewise, the tributary area of the cables can not be neglected during this design stage.

2.5 CABLE ARRANGEMENT

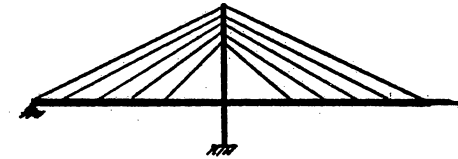
There are four cable configurations utilized by existing cable-stayed bridges (Fig. 6b). The radiating, fan, and harp configurations each have distinct structural advantages. The star configuration, disregarding its load carrying ability, only has aesthetic advantages. Selection of the cable



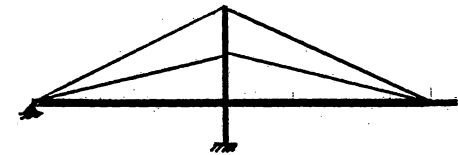
a.)



HARP



FAN



STAR

b.)

Figure 6. Tower configurations and cable configurations.

configuration is dependent on the span length, loads, economy, and the designer's experience and judgement as to which configuration can best be utilized to carry final loads as well as erection loads.

With the radiating or radial configuration, all of the cables converge at the top of the tower. This is an optimum configuration since all cables are at their maximum inclination and support vertical loads with minimum compression in the girder. One disadvantage with this configuration is that high axial compression and lateral forces are concentrated at the top of the tower. Likewise, associated with this problem is that connections at the top of the tower may be difficult with a large number of cables.

The harp system, with parallel cables connecting the girder and tower, provides an optimum tower design. This is achieved by not massing the cable forces at the top of the tower but distributing them along the tower height. The harp system also simplifies connection details since all cables intersect the tower at the same angle. This may also be true on the girder but is dependent on the vertical alignment. Greater aerodynamic stability is also achieved with the harp configuration than with the radiating configuration.

The fan configuration, which is a combination of both the radiating and the harp, exploits the advantages of both configurations while minimizing their disadvantages. The fan configuration provides for an optimum cable inclination while maintaining a vertical distribution of cable force transfer to the tower.

The optimum tower height-to-span ratio (h/L) for the radiating, harp, and fan configuration are 0.29, 0.50, and 0.39 respectively (10). Thus, for the harp configuration a higher tower is needed to exploit its advantages over the other configurations.

The number of cables used on a particular bridge is mainly dependent on loads. Using a few number of cables results in high cable forces as well as large variations in girder moments. Using more cables results in lower cable forces and a better distribution of girder moment and axial force. However, more cables may mean greater cost due to connections.

The number of planes of cables is mainly dependent on the loads and width of roadway required.

2.6 CABLES AND ANCHORAGE SYSTEMS

Current technology has shown that parallel wire strand is the most suitable for cable-stayed bridges. It is far superior to wire rope because (3):

- Strand is stronger than rope of the same diameter.
- Strand has a higher modulus of elasticity.
- Strand is less flexible than rope.

A prestretching procedure is applied to the strand to eliminate the looseness between individual wires in the strand caused during production. This is done to ensure that an accurate modulus of elasticity can be obtained for design purposes.

The modulus of elasticity of a strand ranges from 20,000 ksi to 24,000 ksi. The difference in the modulus is primarily a function of the coating applied to the strand and the diameter of the strand. The greater the diameter the more coating is required to cover the strand. The coating is typically zinc.

Additional corrosion protection, other than zinc, is provided by encasing the cables in steel pipe (PE-Pipe) during erection and injecting cement grout during the final erection stages.

Anchorage of the cables in the bridge deck and the tower is done through the use of HiAm anchorages (7,13). The anchorage allows the high fatigue capacity of parallel wire strand to be utilized (7). The anchorage can be viewed as a socket in which the transfer of cable force is achieved through a plate which bears against a mixture of small steel balls, zinc dust, and epoxy (Fig. 7). At the tower the anchorage can be fixed or, as mentioned previously, saddles can be used.

Data concerning properties used in the design of the cables is generally taken from the manufacturer's published cable properties.

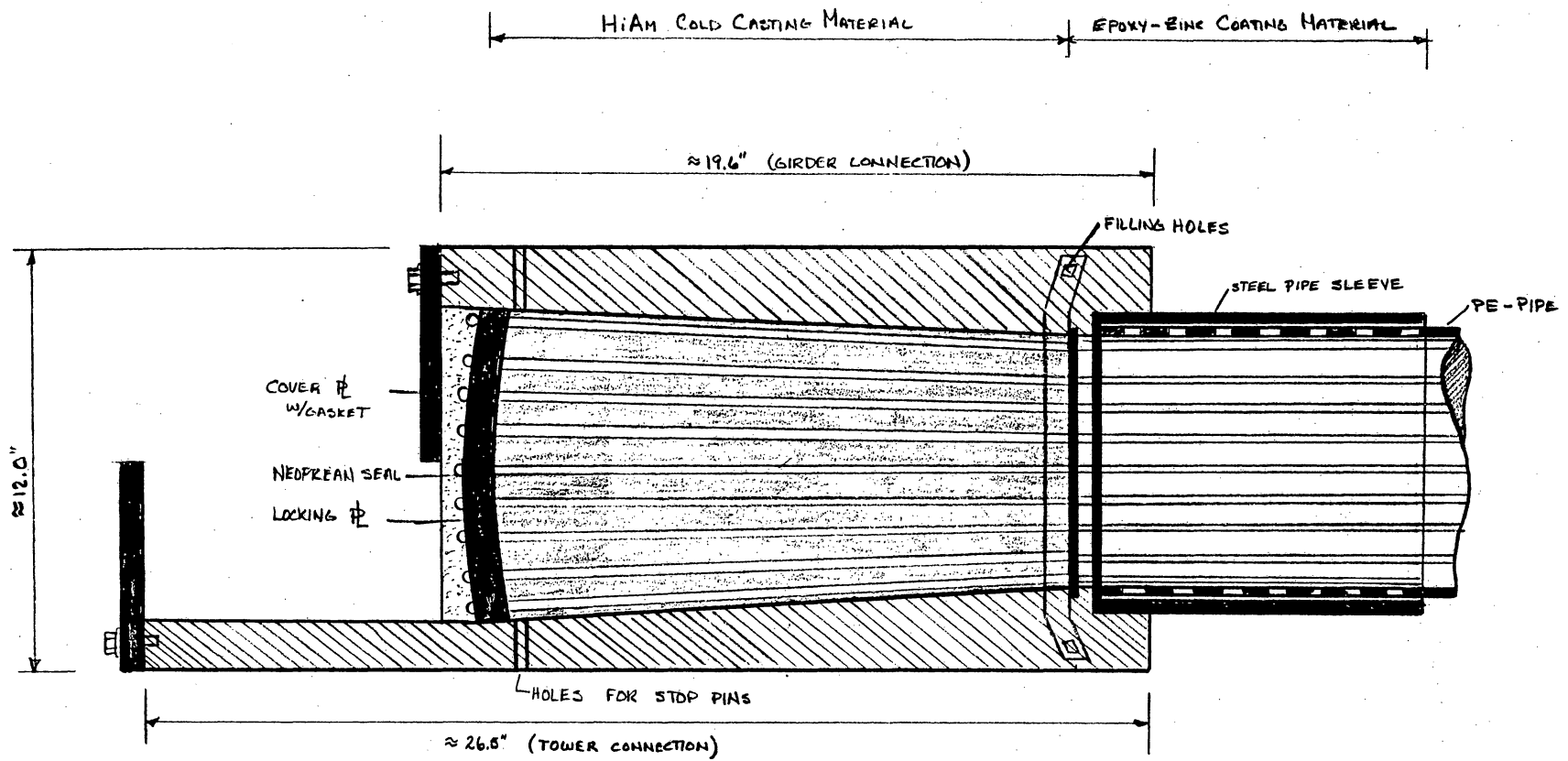


Figure 7. HiAm anchorage system

2.7 POST-TENSIONING

Two tendon post-tensioning patterns are incorporated in the cable-stayed bridge: erection tendons in the upper flange and continuity tendons in the lower flange. Erection tendons in the upper flange counteract negative bending moments at the support and continuity tendons counteract positive bending moments at midspan. The tendons are generally 270 ksi strand.

In designing the post-tensioning, the axial force produced by the cable-stays must not be overlooked. It provides significant compression to counteract tensile stress that result from bending moments in the girder. Tensile stresses can be present at mid span due to cable forces but generally compressive stresses are desired. This can be achieved through proper cable tensioning and cambering of the girder.

CHAPTER 3

A PRELIMINARY DESIGN OF A 600 FOOT MAIN SPAN CABLE-STAYED BRIDGE

3.1 SITE CHARACTERISTICS

A engineering study conducted by the Planing and Research Branch of North Carolina Department of Transportation has determined that a 4 lane fixed span bridge is needed to replace the Washington Baum Bridge over the Roanoke Sound on US-64/264 between Manteo and Nags Head, North Carolina.

The existing bridge, a two lane low level structure founded on treated timber pile bents with a swing span, has an estimated life of 4 years. Excessive deterioration of the bridge deck and pile bents have made repair work to support increased traffic loads and volumes uneconomical. The swing span, likewise, presents problems such as: delays in traffic and constant maintenance costs.

For the replacement, a four lane fixed span bridge with a minimum height and width requirement over the main channel of 65 feet and 90 feet respectively is required. Total projected length of the structure is approximately 5700 feet.

A review of the cost analysis plans for the selected alternative shows a 5652 foot structure with a 1300 foot vertical curve over the main channel with 4% approaches (Fig. 8). Borings at the site reveal that the material under the bridge is mainly fine sand with blow counts taken from the standard penetration test averaging 45 at a depth of 40 feet.

In view of the cost analysis plans, the profile shown in Figure 9 was chosen. Using this profile, a single plane of cables in conjunction with a fixed base cantilever tower and a fan cable arrange-

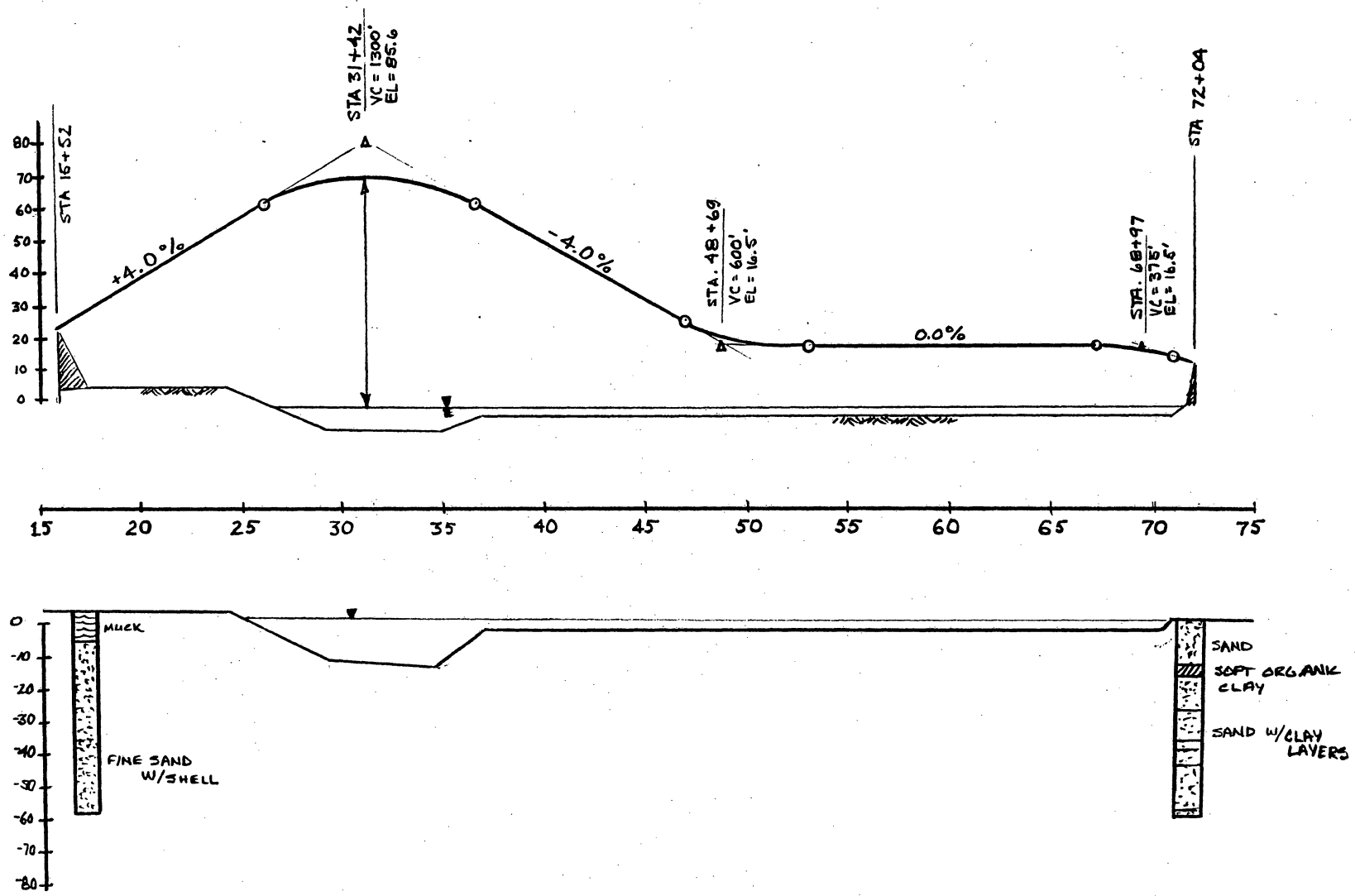


Figure 8. Cost analysis profile and boring log.

ment will be used. Loading will be based on an HS 20 live load due to industrial traffic in the area. Segments will be precast and shipped by barge to the bridge site.

3.2 ASSUMPTIONS MADE FOR THE PRELIMINARY DESIGN

For the longitudinal analysis, the nonlinear behavior of the cable-stayed span will be based on Podolny's theory (section 1.2) that nonlinearity is only associated with the dead load analysis. The live load analysis will be done using linear theory. Using this approach, influence lines may be used in conjunction with the live load analysis to determine the stresses in members for the longitudinal analysis.

As previously stated, the loading will be the HS 20 live load defined by AASHTO. AASHTO states in the introduction that "the requirements apply to ordinary highway bridges and supplemental specifications may be required for unusual types and for bridges with spans longer than 500 feet." Ivey (11), recommends that the following reductions be used for spans in excess of 500 feet (Table 1). These reduced loads have generally been accepted as criteria for loadings on long span bridges. The table also extends the AASHTO loading up to 600 feet.

For transverse loading of the box section, the standard HS 20 truck load will be used once again. Likewise, the requirements for slab design and box girders outlined in AASHTO will be used.

Longitudinal stresses and prestressing will be based on AASHTO specifications for allowable stresses in concrete members.

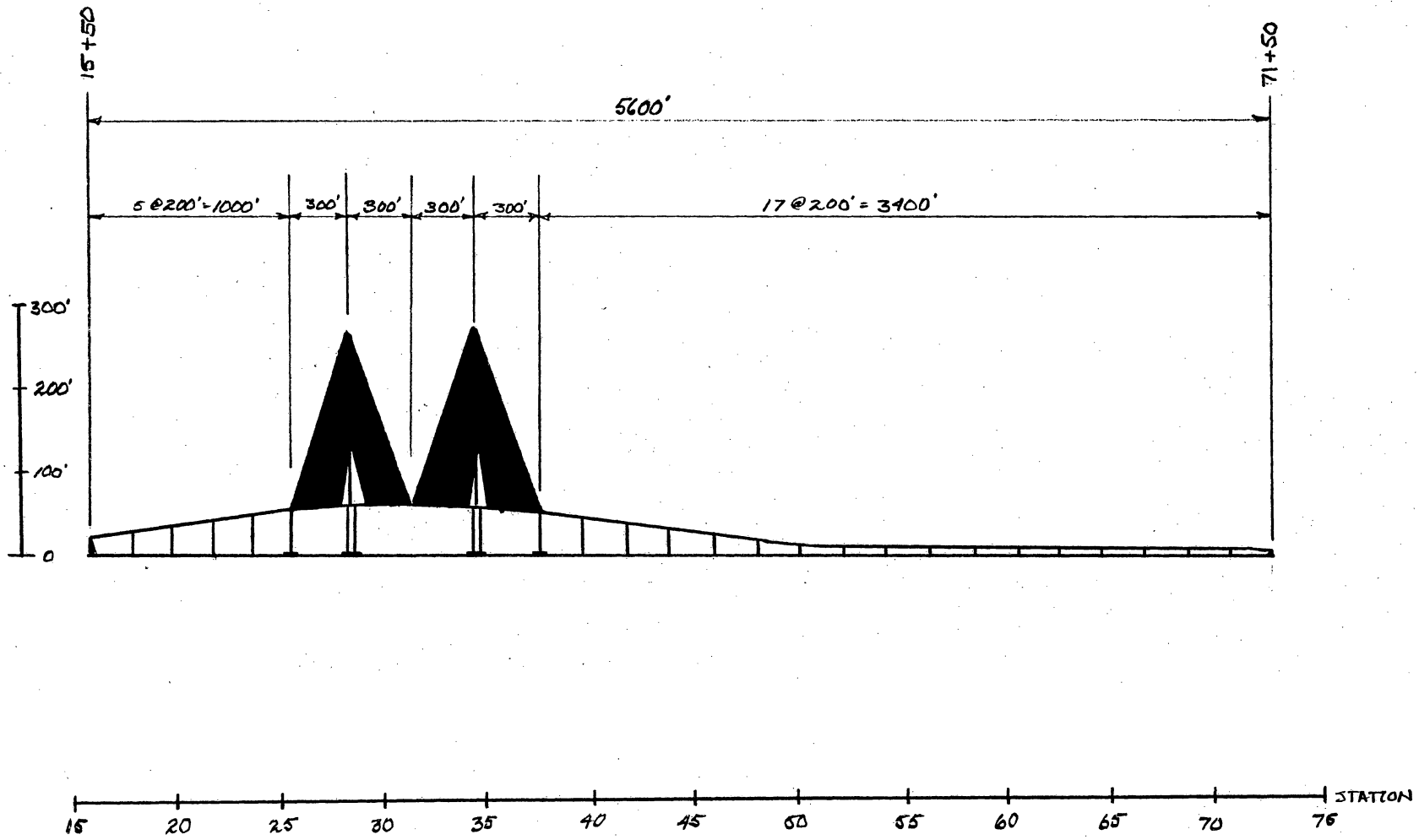


Figure 9. Design profile.

Table 1. Recommended loads for long span bridges.

LOADED LENGTH (ft)	UNIFORM LIVE LOADS (lb/ft)	CONCENTRATED LIVE LOAD MOMENT (lb)	LIVE LOAD SHEAR (lb)
0-600	640	18,000	26,000
601-800	640	9000	13,000
801-1000	640	0	0
1001-1200	600	0	0
1201-OVER	560	0	0

3.3 PRELIMINARY SIZE OF PRECAST SEGMENT CROSS SECTION

The preliminary size of the segment was based on a review of designs of cable-stayed bridges, a study conducted by Kulka (4), AASHTO requirements, and box efficiency as defined by Eq. 2.1.

A. Width of deck

From the cost analysis plans, the proposed cross section specifies 4 traffic lanes 12 feet wide, a median to separate traffic traveling in opposing directions, and a 5 foot shoulder to facilitate guard rails and bicycle traffic are required.

Using these dimensions as guidelines, a width of 66 feet was chosen.

$$\begin{aligned} \text{Central median to facilitate tower and guard rails} &= 8' \\ 4 \text{ lanes @ 12 feet} &= 48' \\ 2 \text{ shoulders @ 5 feet} &= 10' \\ \text{Total Width} &= 66' \end{aligned}$$

With a width greater than 40 feet a single cell box girder with interior brace and a multicell box girder were investigated (Fig. 10). Based on their efficiency and apparent ease in construction, the single cell box was chosen.

B. Top slab thickness

AASHTO recommends a top slab thickness for box girders of (Eq. 3.1)

$$\frac{(S + 10)}{20} \tag{3.1}$$

where, S = the center to center spacing of webs.

With the single cell box girder, an S equal to 22 feet was used instead of the distance between webs of 44 feet. This was done based on the interior brace acting as a support and thickening of the top slab at the center. Based on this assumption, a top slab thickness of 19.2 inches is required. Since fillets are required at the intersection of slab and web, a stiffer slab is provided. Because of

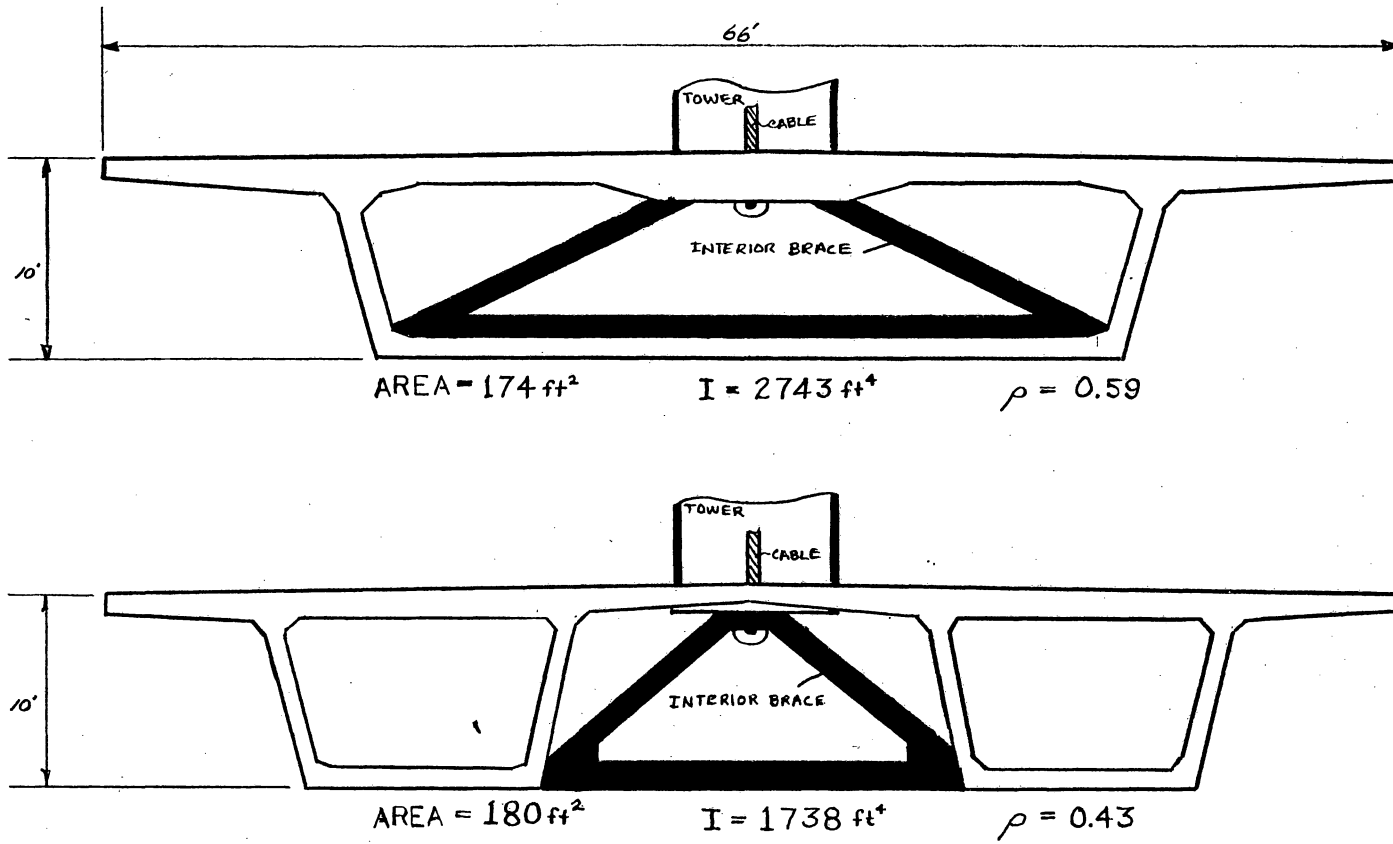


Figure 10. Single cell and multi box girder comparison.

this, the slab thickness was reduced to 16.2 inches (The deflection of the slab in this region was checked and proved not to be critical. Maximum deflection at this point was 0.02 inches.).

C. Cantilever length and thickness

A 12 foot cantilever was chosen to limit the thickness required at the intersection of the web. From Kulka's study, a depth at the intersection of the cantilever and the web is defined by the following equation (Eq. 3.2).

$$0.064(L) + 0.814 \quad (3.2)$$

where L = cantilever length in feet. With a cantilever length of 12 feet, this corresponds to a depth of 18.9 inches.

D. Depth of section

Based on a review of cable-stayed bridges, a span-to-depth ratio of 1:60 was chosen. This is also based on aesthetics with the approach span, where, from Kulka's study, a recommendation of depth defined by the following equation (Eq. 3.3) yields a depth of 8.85 feet ($L = 200$ ft.).

$$0.042(L) + 0.45 \quad (3.3)$$

The depth was increased to 10 feet to take advantage of the increased moment of inertia and increased lever arm for prestressing design.

E. Bottom flange width and thickness

AASHTO states that "the thickness of the bottom slab of a box girder shall not be less than 1/16 of the clear span between girder webs or 5.5 inches, except that the thickness need not be greater than the top slab unless required by design." The recommendation proposed by Kulka for bottom slab thickness and width is defined by the following equation (Eq. 3.4).

$$ST(SW/W) = 0.005(L) - 0.654 \quad (3.4)$$

where:

ST = Bottom slab thickness

SW = Bottom slab width

W = Deck width

Using top flange cantilevers of 12 feet and a web batter of 1:4, results in a bottom slab width of 38 feet. Solving for ST in Eq. 3.4 results in a thickness of 7.21 inches. Since this cannot be smaller than the top slab thickness of 16.2 inches, a thickness of 16.25 inches will be used.

F. Web thickness

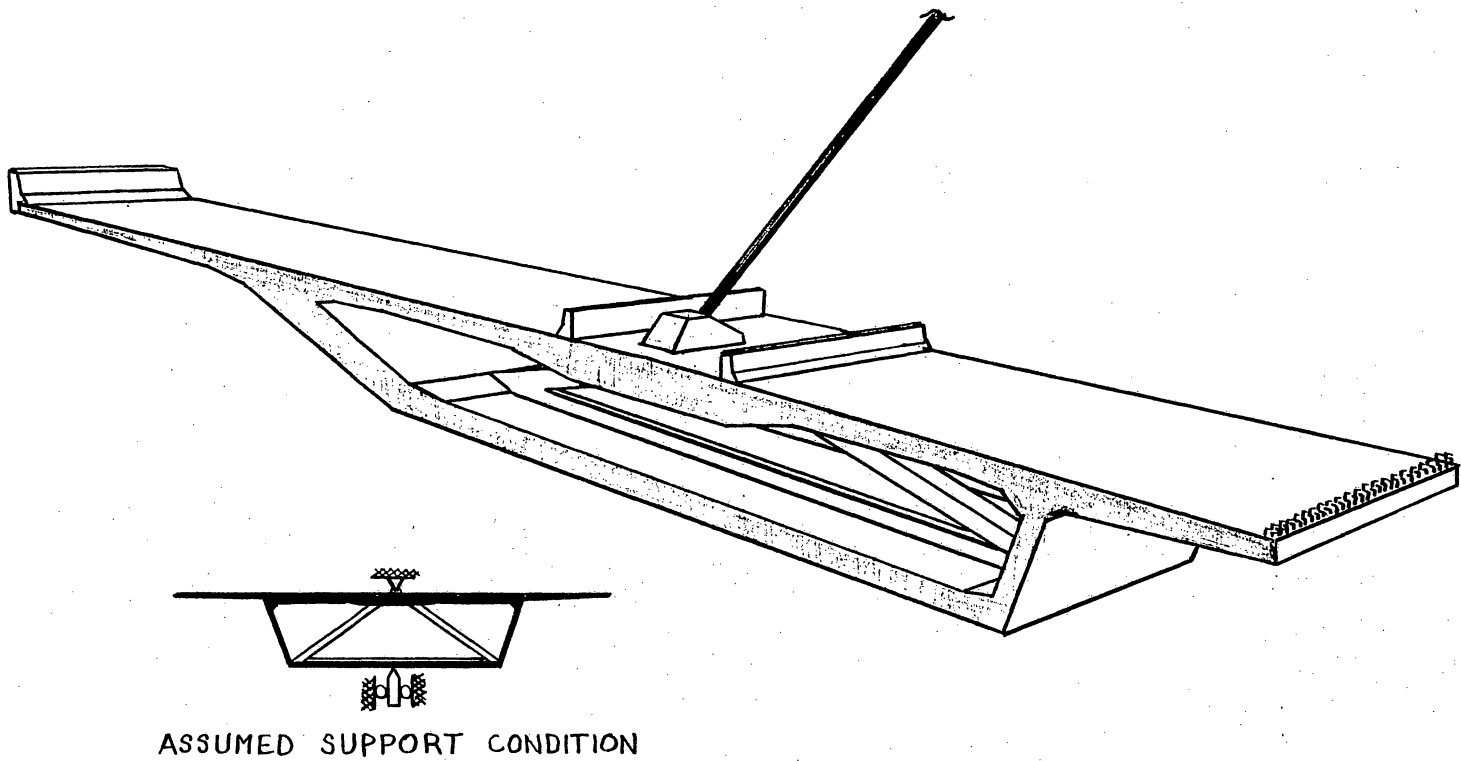
AASHTO has no requirements for web thickness. Podolny and Muller (11) recommend a minimum thickness of 12 inches when prestressing tendon ducts occur in the web.

Summary of segment cross section dimensions

In view of the minimum widths and thicknesses previously determined, the following dimensions, as shown in Figure 11, were chosen for the design. All fillets and tapered sections were incorporated in the calculations of the area and moment of inertia, however, the interior brace was not. Allowances for vehicular traffic to bear directly on the top slab have been allotted for, as well as, a crown of a 1/4 inch per foot.

3.4 TRANSVERSE ANALYSIS OF THE BOX SECTION

The transverse deck was analyzed using the AASHTO recommendations for the distribution of loads for the design of concrete slabs. From these loads, the box was analyzed as a frame. The support of the box was assumed to range from a multiple support under the bottom slab (pier support) to a single attachment at the center of the top (cable attachment) as depicted in Figure 12 and Figure 13. The interior brace was assumed to act as truss elements since it provided very



ASSUMED SUPPORT CONDITION

Figure 12. Typical cable segment with cable-stay attachment.

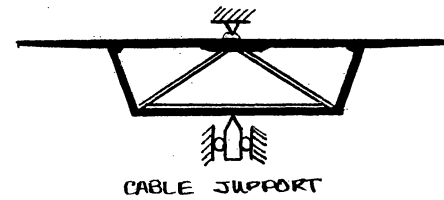
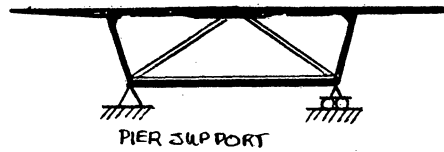
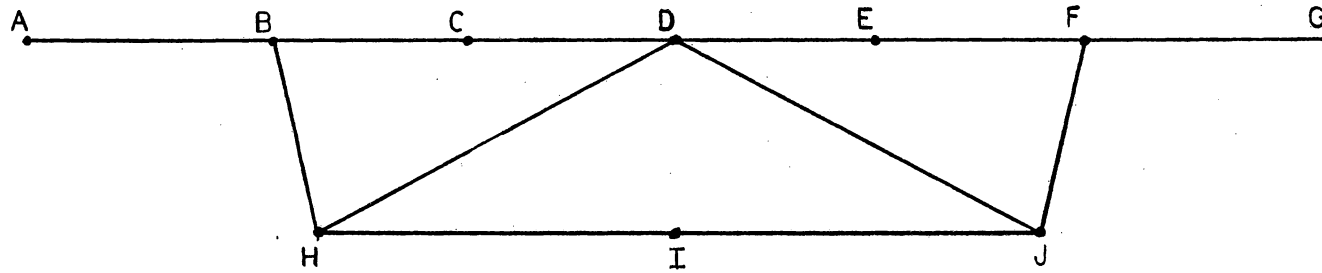


Figure 13. Line diagram for moment reference and assumed support conditions.

little moment restraint at the joints as compared to the elements it framed into. Since AASHTO requires that the fillets be included in the analysis, they were modeled as a series of small elements depicting the taper.

The dead load analysis included a solid concrete guard rail similar to a New Jersey median barrier at the cantilever ends weighing 0.62 kips/foot. Results of the dead load analysis of each support condition were superimposed to get dead load moment envelopes for the members of the box section (Fig. 14).

The live load analysis was based on a HS 20 truck load and live load moment for simple spans given by Equation 3.5 with the continuity factor of 0.8 for spans continuous over 3 or more supports.

$$\left[\frac{S + 2}{32} \right] P_{20} \quad (3.5)$$

The live load analysis considered unsymmetrical load patterns to cause maximum stresses in the top slab at critical sections. Again, as was done with the results of the dead load analysis, the results of the live load analysis based on the two support conditions were superimposed to get one live load moment envelope (Fig. 15).

The following calculations were used to determine loads to perform the frame analysis and the reinforcement in the transverse and longitudinal direction.

Top slab moment per linear foot:

$$M = \left[\frac{22 + 2}{32} \right] (16)(0.8) = 9.6 \text{ k-ft}$$

Cantilever moment per linear foot:

$$\begin{aligned} E_1 &= 0.8(10.5) + 3.75 = 12.15 \text{ ft} \\ E_2 &= 0.8(4.5) + 3.75 = 7.35 \text{ ft} \\ M &= \frac{16}{12.15}(10.5) + \frac{16}{7.35}(4.5) = 23.62 \text{ k-ft} \end{aligned}$$

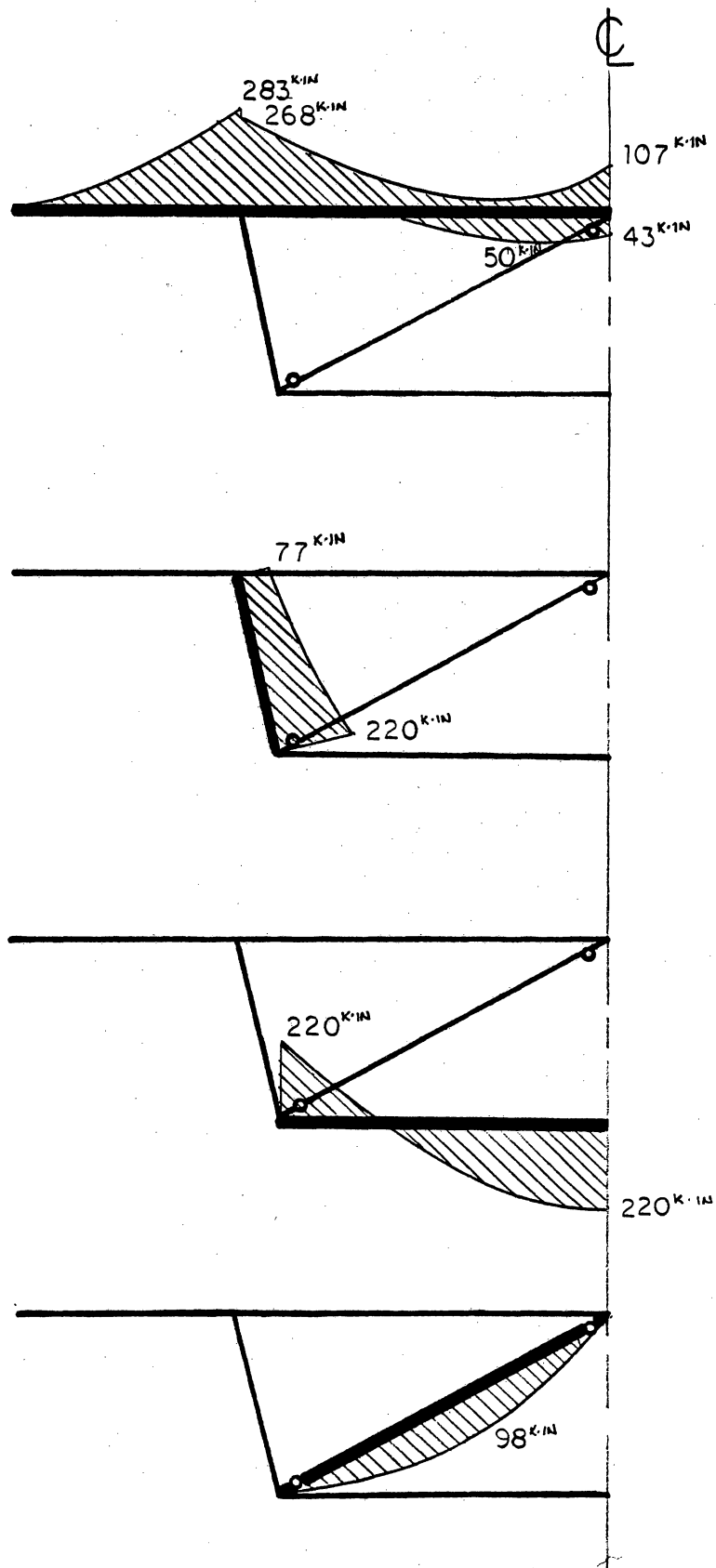


Figure 14. Dead load moment envelope, superimposing the support conditions.

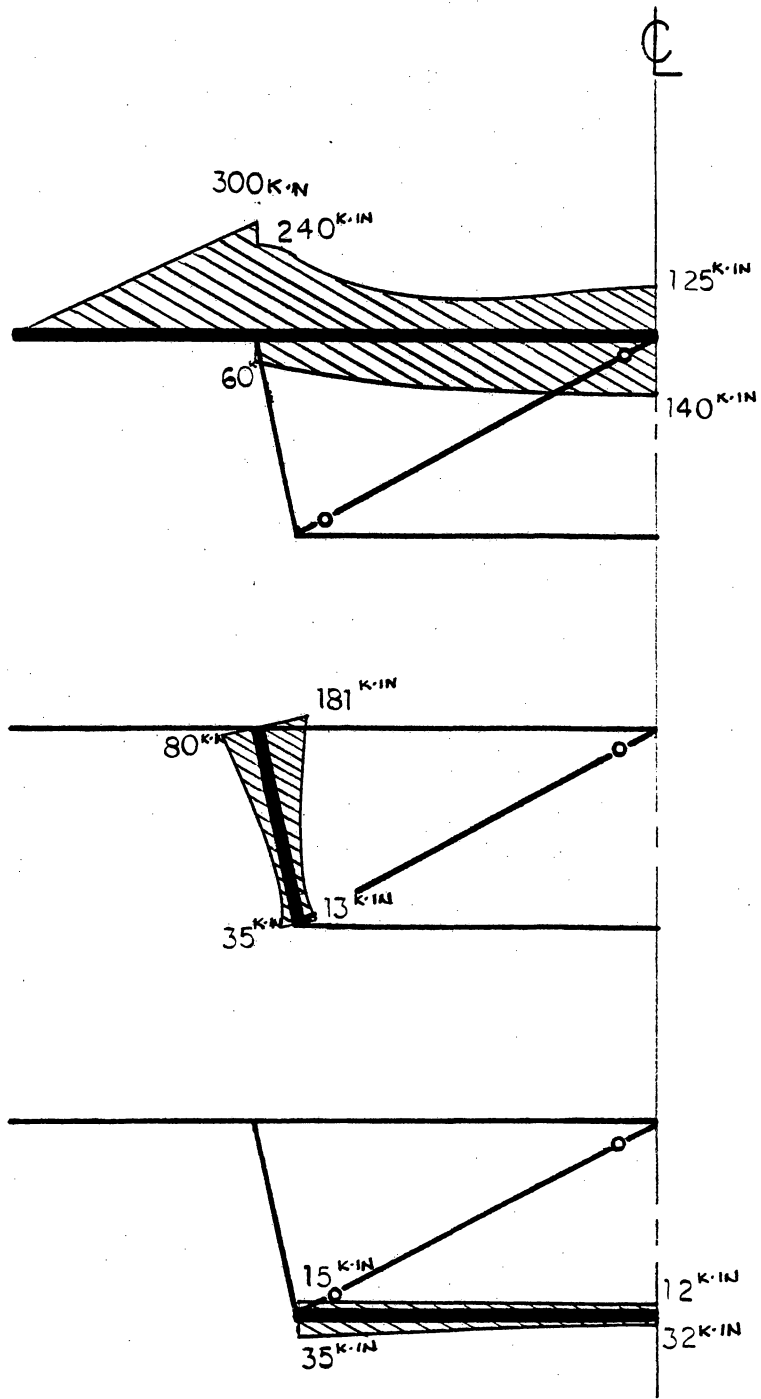


Figure 15. Live load moment envelope, superimposing the support conditions.

Table 2. Ultimate transverse positive and negative moment tabulation.

$$MU = 1.3[MDL + 1.67(MLL + MI)]$$

MEMBER	LOCATION	MDL(k-ft)	MLL(k-ft)	MI(k-ft)	MU(k-ft)	
Top Slab	B/BA	-23.5	-25.0	-7.5	-101.1	
	B/BC	22.3	20.0	6.0	85.4	
	C/CB	-1.0	-8.0	-2.4	-23.9	
	D/DC	-8.9	-10.4	-3.1	-40.9	
	B/BA	-23.5	-	-	-30.6	
	B/BC	17.1	-5.0	-1.5	36.0	
	C/CB	6.6	8.0	2.4	31.2	
	D/DC	3.6	11.7	3.5	37.7	
	Webs	B/BH	1.2	-6.6	-17.1	-17.1
		H/HB	-18.3	-2.9	-0.9	-15.6
		B/BH	18.3	1.3	0.4	50.7
		H/HB	18.3	-1.0	-0.3	27.5
	Bottom Slab	H/HI	18.3	-2.9	0.9	15.6
		I/IH	15.0	1.0	0.3	22.3
H/HI		18.3	1.3	0.4	15.6	
I/IH		18.3	-1.0	-0.3	21.0	

Note: The difference in dead load moment is due to the different support conditions.

Selection of reinforcing steel was based on a concrete strength of 5000 psi and grade 60 reinforcing steel. Bars located in the top of the top slab will be epoxy coated to inhibit corrosion. The following calculations were used to determine the steel area required at critical sections and to select bar sizes.

A. Cantilever

B/BA:

$$d = 21'' - 2'' - 0.75'' = 18.3 \text{ in}$$

$$MU = 123 \text{ k-ft}$$

$$R_u = \frac{(101)(12)}{(0.9)(12)(18.3)^2} = 0.335 \text{ ksi}$$

$$\rho = 0.0058$$

$$A_s = 0.0058(12)(18.3) = 1.27 \text{ in}^2/\text{ft}$$

$$\#10 \text{ @ } 12 \text{ inches o.c., } A_s = 1.27 \text{ in}^2/\text{ft}$$

Checking crack control

$$l_d = 43.12(1.4) = 60.35 \text{ in}$$

$$n = 7, \rho = 1.27, j = 0.916, jd = 16.77 \text{ in}$$

$$f_s = \frac{(23.5 + 25.0 + 7.5)(12)}{(16.77)(1.693)} = 23.66 \text{ ksi} < 0.6f_y$$

$$z = (23.66)[(2.625)(47.25)]^{1/3} = 117.99 \text{ k/in}$$

B. Top slab

B/BC 5 feet from B:

$$d = 16.2'' - 2'' - 0.75'' = 13.45 \text{ in}$$

$$MU \cong 65 \text{ k-ft}$$

$$R_u = \frac{(65)(12)}{(0.9)(12)(13.45)^2} = 0.399 \text{ ksi}$$

$$\rho = 0.0066$$

$$A_s = 0.0066(12)(13.45) = 1.07 \text{ in}^2/\text{ft}$$

$$\#10 \text{ @ } 12 \text{ inches o.c., } A_s = 1.27 \text{ in}^2/\text{ft}$$

D/DC, Note: Positive and negative moment are approximately the same.

$$d = 21'' - 2'' - 0.75'' = 18.3 \text{ in}$$

$$MU = 41 \text{ k-ft}$$

$$R_u = \frac{(41)(12)}{(0.9)(12)(18.3)^2} = 0.1367 \text{ ksi}$$

$$\rho = 0.0023$$

$$A_s = 0.0023(12)(18.3) = 0.51 \text{ in}^2/\text{ft}$$

$$\#9 @ 18 \text{ inches o.c. interior and exterior, } A_s = 0.66 \text{ in}^2/\text{ft}$$

C/CB, Note: Positive and negative moment are approximately the same.

$$d = 16.2'' - 2'' - 0.75'' = 13.45 \text{ in}$$

$$MU = 24 \text{ k-ft}$$

$$R_u = \frac{(24)(12)}{(0.9)(12)(13.45)^2} = 0.147 \text{ ksi}$$

$$\rho = 0.0027$$

$$A_s = 0.0027(12)(13.45) = 0.44 \text{ in}^2/\text{ft}$$

$$\#9 @ 18 \text{ inches o.c. interior and exterior, } A_s = 0.66 \text{ in}^2/\text{ft}$$

C. Webs

B/BH Exterior:

$$d = 14'' - 2'' - 0.5'' = 11.5 \text{ in}$$

$$MU = 17.1 \text{ k-ft}$$

$$R_u = \frac{(17.1)(12)}{(0.9)(12)(11.5)^2} = 0.144 \text{ ksi}$$

$$\rho = 0.0025$$

$$A_s = 0.0025(12)(11.5) = 0.345 \text{ in}^2/\text{ft}$$

$$\#7 @ 15 \text{ inches o.c., } A_s = 0.48 \text{ in}^2/\text{ft}$$

B/BH Interior:

$$d = 14'' - 2'' - 0.5'' = 11.5 \text{ in}$$

$$MU = 50.7 \text{ k-ft}$$

$$R_u = \frac{(50.7)(12)}{(0.9)(12)(11.5)^2} = 0.426 \text{ ksi}$$

$$\rho = 0.0085$$

$$A_s = 0.0085(12)(11.5) = 1.173 \text{ in}^2/\text{ft}$$

$$\#9 @ 9 \text{ inches o.c.}, A_s = 1.33 \text{ in}^2/\text{ft}$$

H/HB Interior:

$$d = 14'' - 2'' - 0.5'' = 11.5 \text{ in}$$

$$MU = 27.5 \text{ k-ft}$$

$$R_u = \frac{(27.5)(12)}{(0.9)(12)(11.5)^2} = 0.231 \text{ ksi}$$

$$\rho = 0.0032$$

$$A_s = 0.0032(12)(11.5) = 0.44 \text{ in}^2/\text{ft}$$

$$\#7 @ 15 \text{ inches o.c.}, A_s = 0.48 \text{ in}^2/\text{ft}$$

D. Bottom slab

H/HI and I/IH:

$$d = 14'' - 2'' - 0.75'' = 11.25 \text{ in}$$

$$MU = 22.3 \text{ k-ft}$$

$$R_u = \frac{(22.3)(12)}{(0.9)(12)(11.25)^2} = 0.196 \text{ ksi}$$

$$\rho = 0.0033$$

$$A_s = 0.0033(12)(11.25) = 0.445 \text{ in}^2/\text{ft}$$

$$\#7 @ 15 \text{ inches o.c. top and bottom}, A_s = 0.48 \text{ in}^2/\text{ft}$$

Reinforcement summary

Figure 16 summarizes the reinforcement to be placed in the transverse direction.

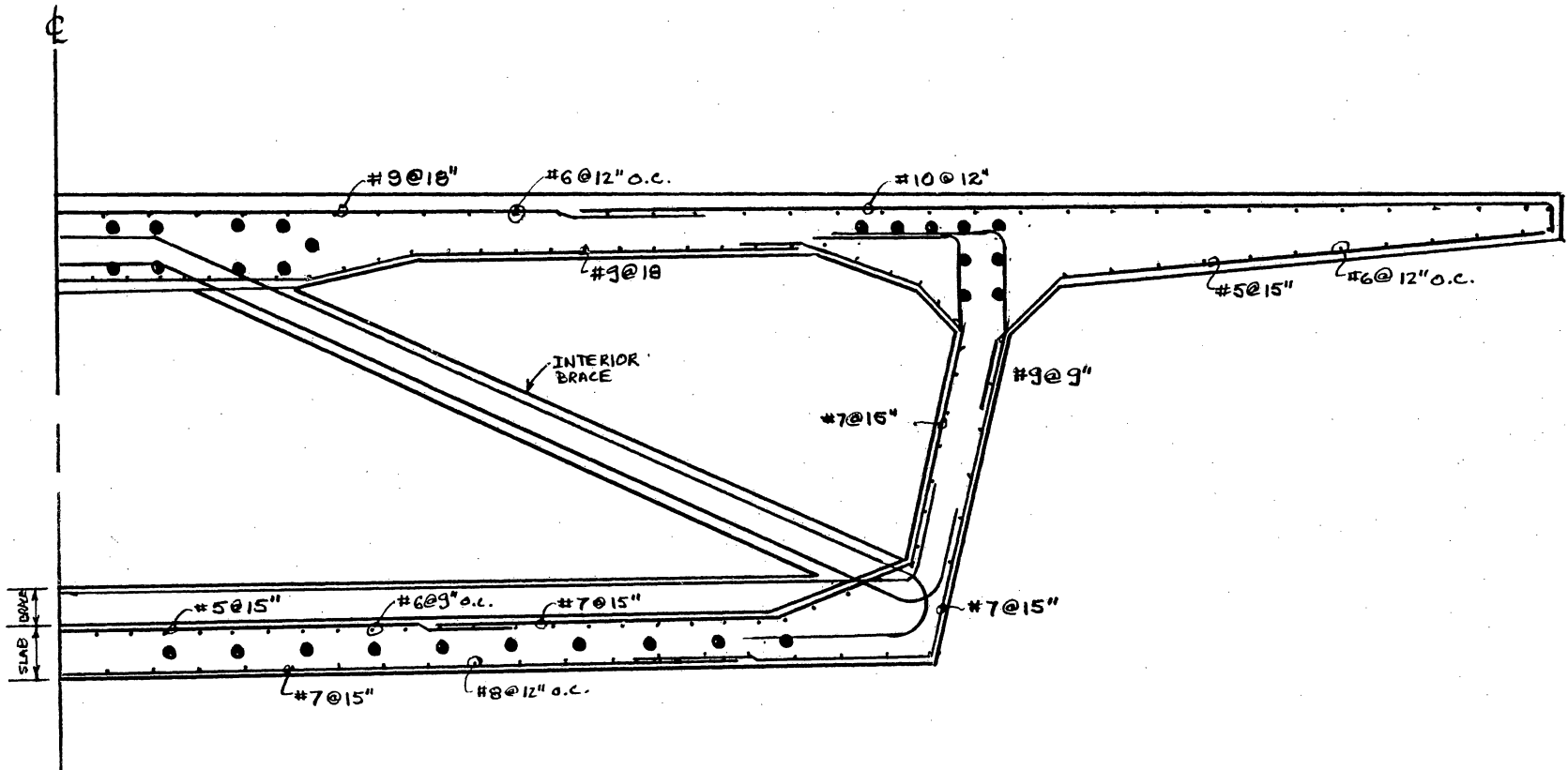


Figure 16. Reinforcement detail.

3.4 MAIN TOWER AND CABLE-STAY DESIGN

To exploit the advantages of the fan cable configuration a tower-to-span ratio of 0.39 should be used. With a span of 600 feet, this results in a tower height of 234 feet. For aesthetic reasons, this will be shortened to 210 feet so that the tower will not appear to overpower the structure. This reduces the tower-to-span ratio to 0.35. The tower will be comprised of hollow rectangular elements with outside dimensions at the base of 15 feet by 7.5 feet tapering to 8 feet by 7.5 feet at the top (Fig. 17). Cables will be anchored in the tower using HiAm anchorage connections.

Cable-stay sizes were selected using an iterative procedure in which:

1. A sag ratio was estimated dependent on the cable size and limiting the stress in the cable to approximately 45 percent of the ultimate.
2. Horizontal and vertical forces produced by the cable weight were calculated using catenary equations (Eq. 1.1-1.5) and the coordinate geometry of the structure.
3. These forces were then applied to the structure at the joints where the cables were connected.
4. Using ABAQUS (2) (finite element analysis program) and the Newton-Raphson nonlinear geometry option associated with the program, the dead weight (Girder: 26.0 k/ft) was applied in thirty increments to the structure in its completed configuration to determine the stresses in the elements. The cable elements were modeled as truss elements with a modulus of elasticity of 23,000 ksi. They were assumed to resist compression through a reduction in prestress.
5. If little or no residual stresses existed in the elements modeling the cables, then the initial guess of the sag ratio was assumed to be correct. The stress in the cable was assumed to be that

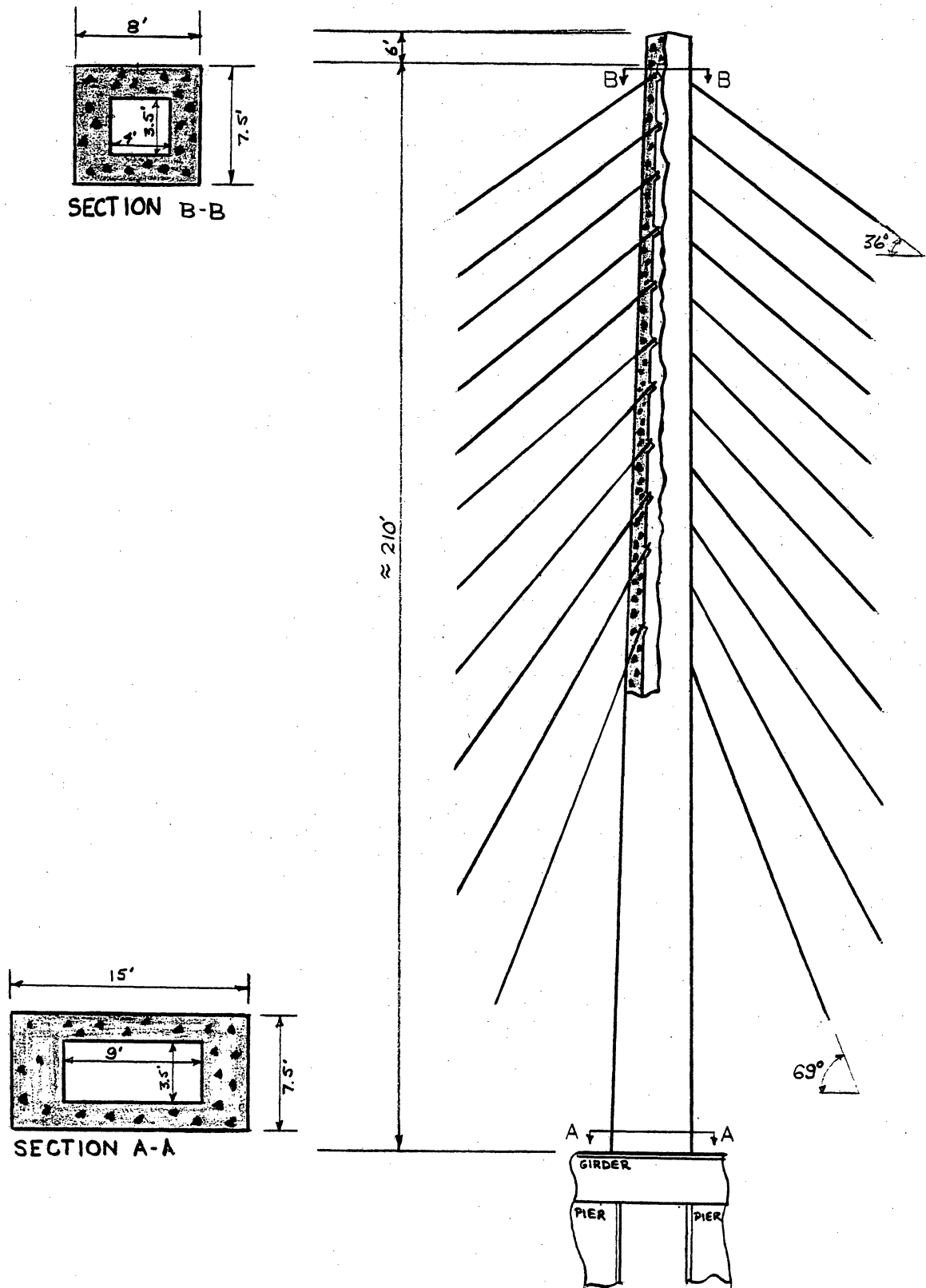


Figure 17. Tower detail.

required to achieve the assumed sag ratio. Displacements of the tower and girder were also checked to ensure they were not excessive.

Using this procedure, a steel cable area of 12.7 square inches was very close to satisfying the stress requirement suggested by Tang (14) of limiting the stress to 40 to 45 percent of the ultimate strength of 200 ksi (Table 3). Using a sag ratio of 1/500 and a larger cable area produces axial tension stresses in the girder at mid span. Likewise, this corresponds to a sag ratio of approximately 1:500, which, in reference to Figure 1, is in the range where the equivalent modulus of elasticity approximates the true modulus of elasticity. This confirms using the true modulus during the analysis for the selection of stay sizes was a valid assumption. In view of the results, the cables will be 4.75 inches in diameter (Note: The steel area of cables is approximately 76 percent of that computed using the area of a circle).

Application of the live load on the structure produced very little change in stress in the cables. The live load analysis was done using linear theory in accordance with Podolny's assumption previously stated. When the structure was fully loaded with the lane load and a point load, the critical cable (cable 19) underwent a stress change of only 5.47 ksi. This is approximately 6 percent of the recommended design value of 45 percent of the ultimate strength. The small change in stress is due to a live load-to-dead load ratio of approximately 1:14 (live load considered here is the uniform lane load of 640 lbs/ft/lane considering the 75 percent reduction factor for four lanes of traffic as depicted in AASHTO). Tang, also states that for long span bridges the live load rarely reaches 60 percent of the design value.

Table 3. Cable length, inclination, end forces, and stresses.

Cable numbers refer to Figure 18.

$$\eta = 1/500$$

CABLE NUMBER	ANGLE (Degrees)	CHORD LENGTH(ft)	H (kips)	V_B (kips)	V_T (kips)	σ_{max} (ksi)
1	36	368.2	1017.1	744.4	760.6	100.0
2	38	337.6	932.6	721.4	736.4	93.5
3	39	311.4	860.2	695.6	709.4	87.8
4	44	283.8	784.1	674.1	686.6	82.1
5	42	285.3	713.5	652.9	664.3	76.8
6	45	232.5	642.2	639.9	647.2	71.8
7	47	206.7	571.0	629.1	638.2	67.4
8	51	181.5	501.5	634.8	642.8	64.2
9	55	158.8	438.7	654.4	661.5	62.5
10	61	137.8	380.7	708.7	714.8	63.7
11	69	118.3	326.8	879.5	884.7	74.3
12	69	116.6	322.2	853.2	858.4	72.2
13	61	135.2	373.5	682.5	688.4	61.7
14	55	155.2	465.9	626.9	633.8	60.3
15	51	177.1	489.2	604.2	612.0	61.7
16	47	199.9	552.1	769.8	609.6	64.7
17	45	223.1	616.2	608.4	618.2	68.7
18	42	247.0	682.3	621.3	632.2	73.2
19	40	271.1	748.7	638.8	650.7	78.1
20	39	295.9	817.6	657.9	671.0	83.3
21	38	321.2	891.1	689.9	704.2	89.4
22	36	346.2	956.4	702.4	717.7	94.2

3.5 DEVELOPMENT OF LONGITUDINAL SHEAR AND MOMENT ENVELOPES

The analysis of the longitudinal bending stress was performed using Podolny's theory of the nonlinearity associated with cable-stayed bridges. The cables were assumed to resist compressive stress through the release of prestress force.

For the analysis of dead load stresses, the forces produced by the cables determined previously (Table 3) during cable selection were applied to the structure in conjunction with the dead load of all elements. Tapered elements were broken into smaller sub elements which were varied in size to approximate the taper. Symmetry was exploited during application of the dead load. The structure, with its support conditions, was modeled as depicted in Figure 18. Stresses in the girder produced by the dead load of the structure are depicted in Figure 19 and are symmetric about the center line.

For the live load analysis, the complete structure was used so that unsymmetrical load patterns could be analyzed. The live load analysis was done using linear theory.

To determine the maximum live load stress in the girder, influence lines were developed to determine the load patterns governing maximum stresses in the members (Fig. 20). Once this was done, the uniform lane load of three lanes (AASHTO lane loads using reduction factor of 75 percent for four lanes) was applied to the structure to produce maximum positive and negative stresses in the members. The point load of 54 kips for moment and 78 kips for shear were multiplied by the influence ordinates to cause the maximum stresses in the member. Likewise, this was done in accordance with AASHTO requirements for continuous spans. From this analysis, live load moment and shear envelopes were determined (Fig. 21). Axial force produced in the members during the analysis was negligible in comparison with that produce by the dead load and was ignored for any further calculations.

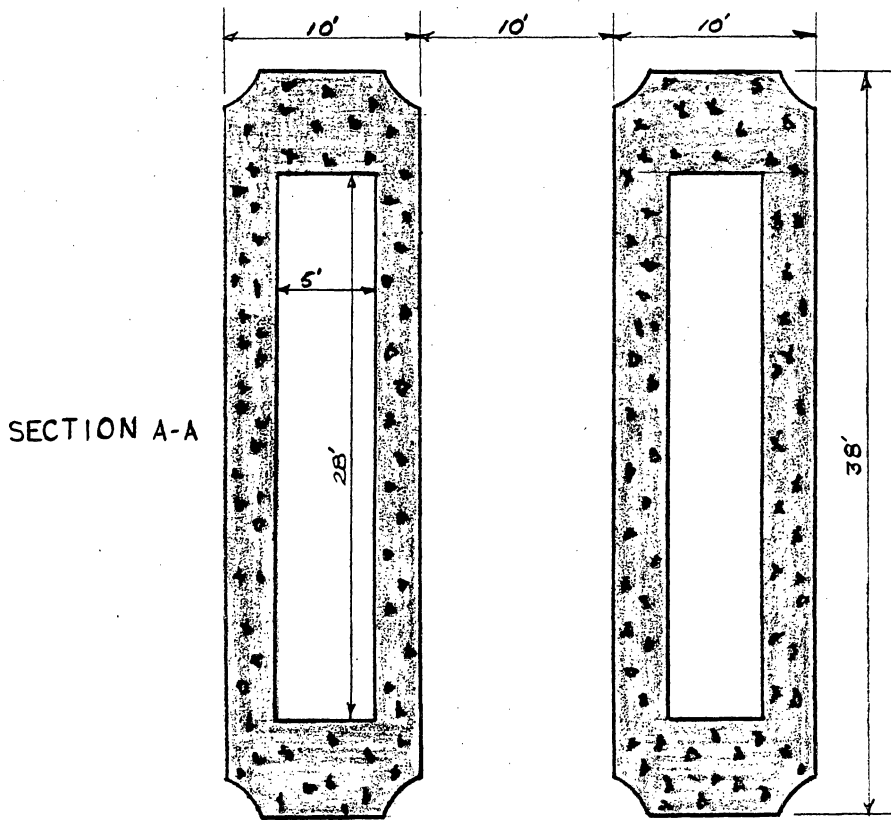
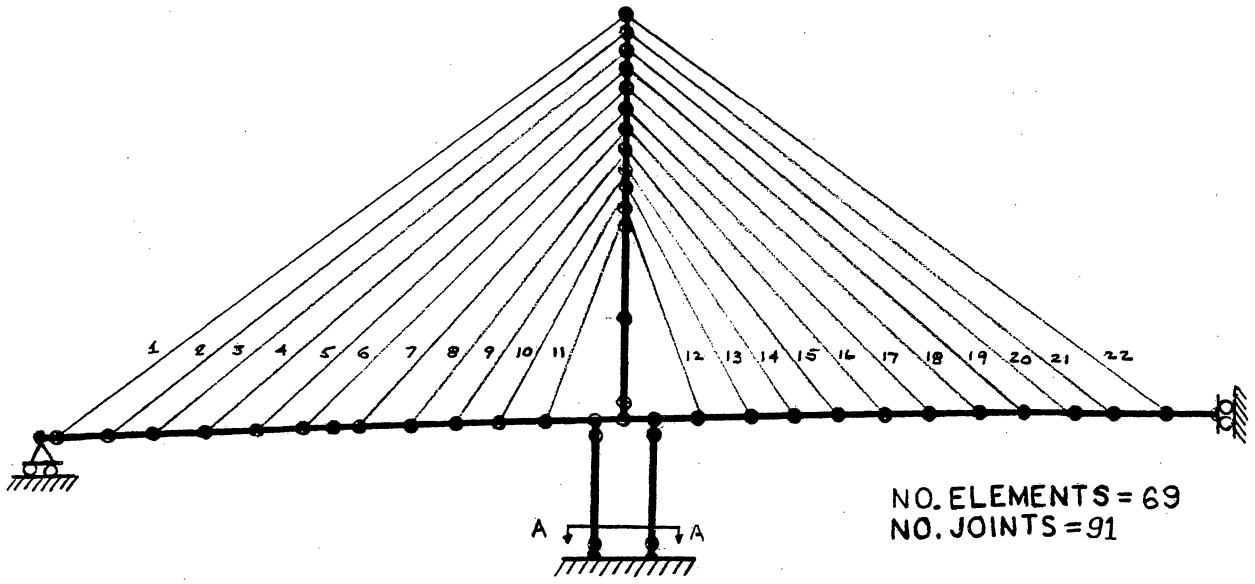


Figure 18. Model of structure used to perform dead load analysis.

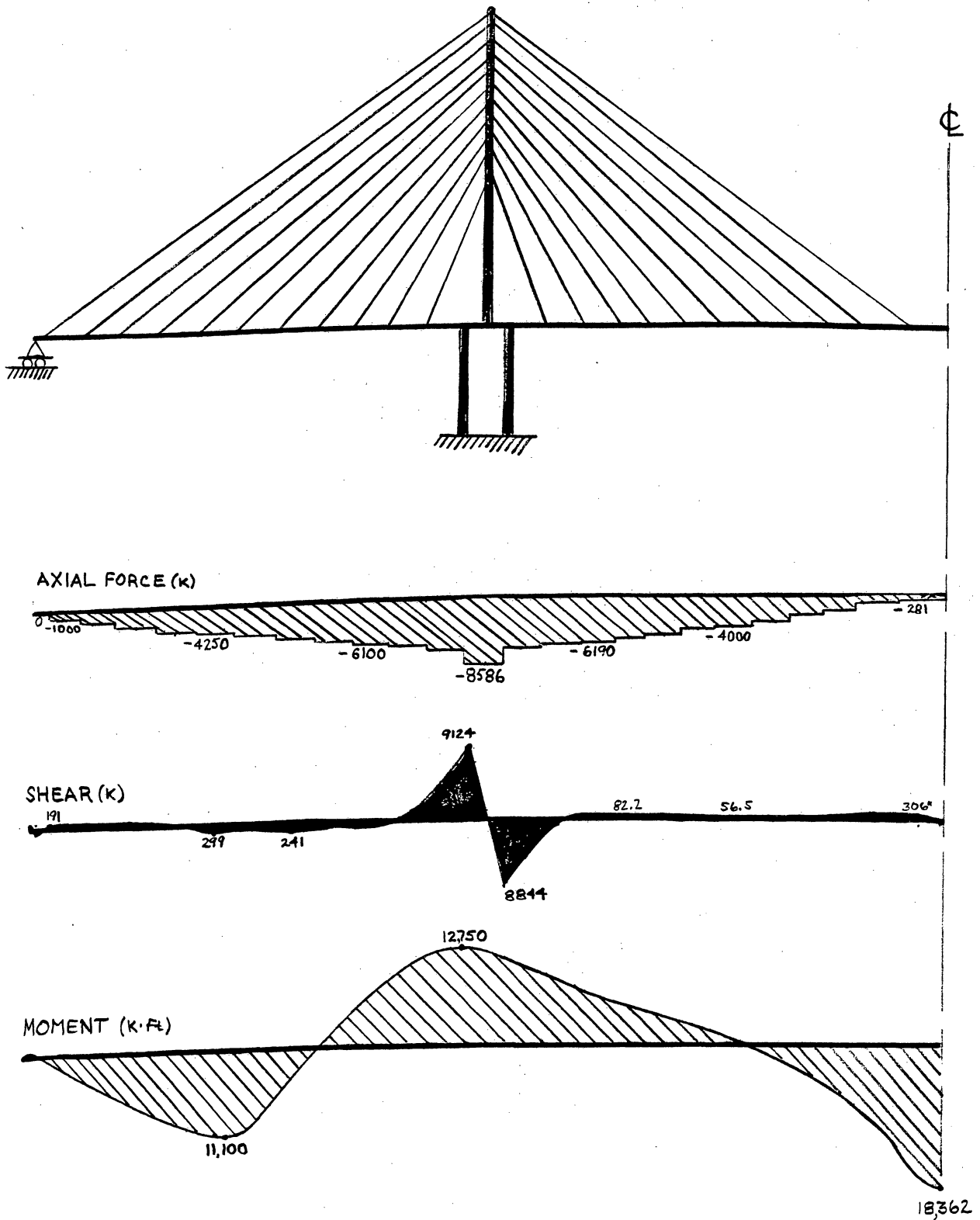


Figure 19. Dead load axial force, shear, and moment in the girder.

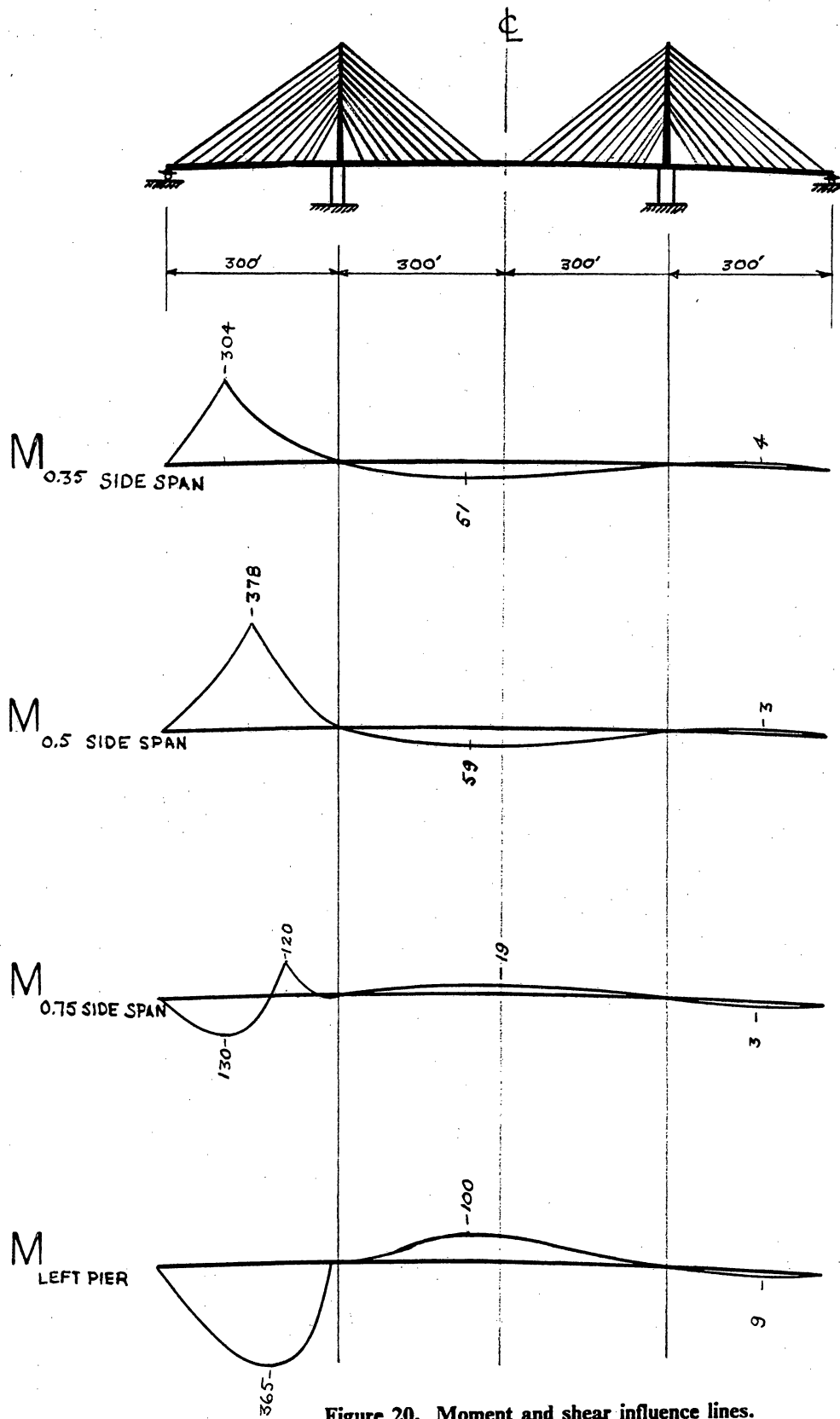


Figure 20. Moment and shear influence lines.

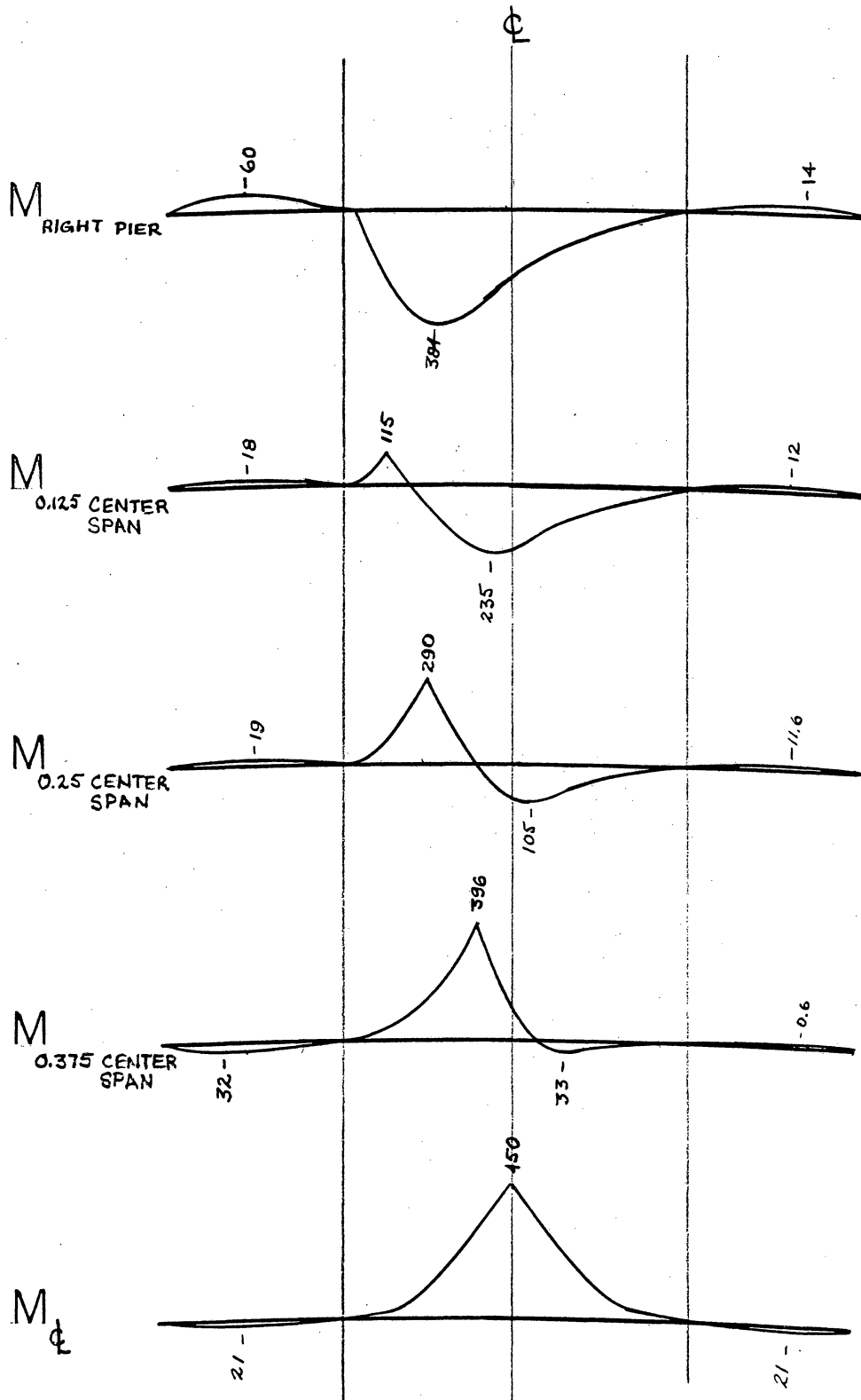


Figure 20. Continued.

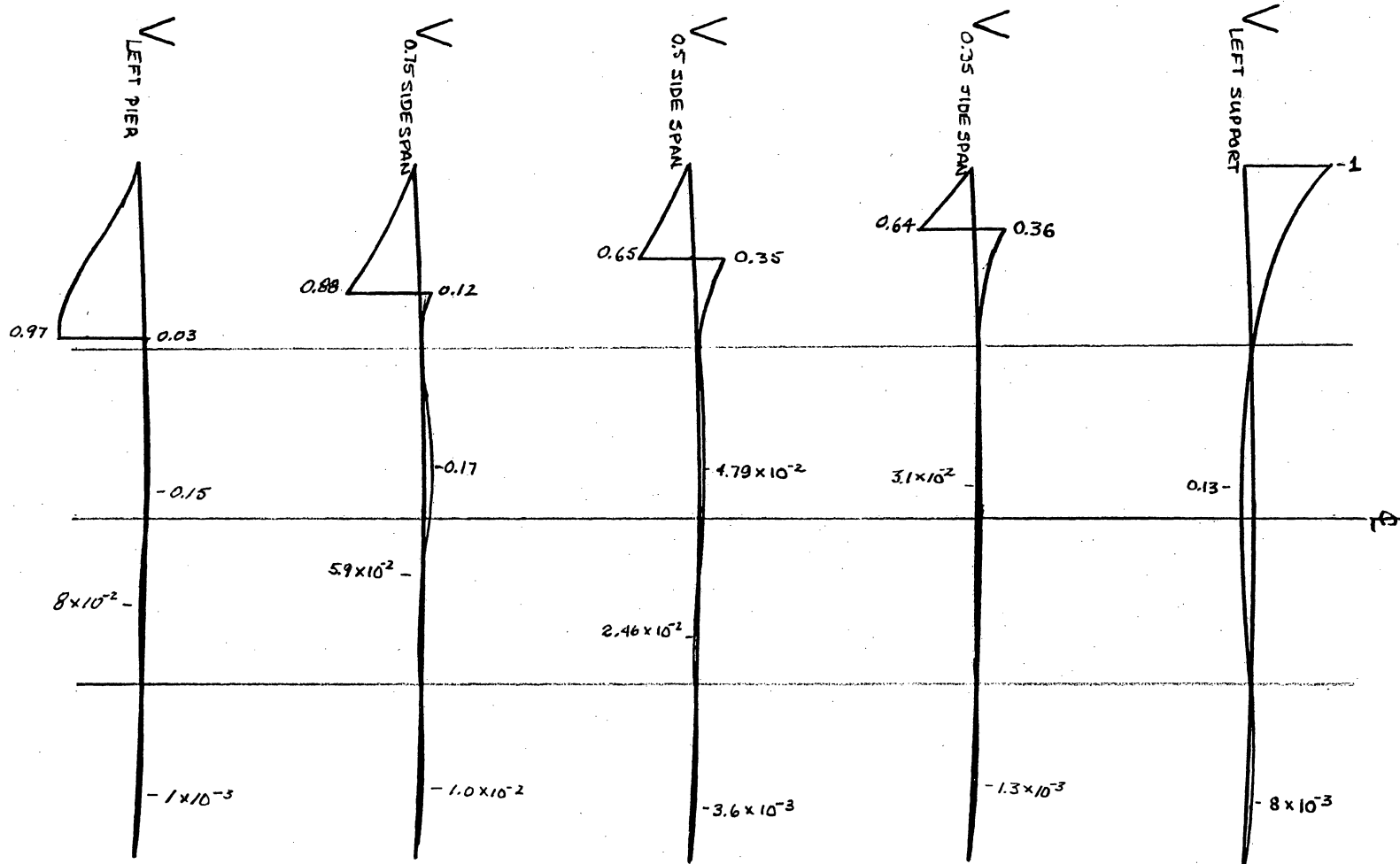


Figure 20. Continued.

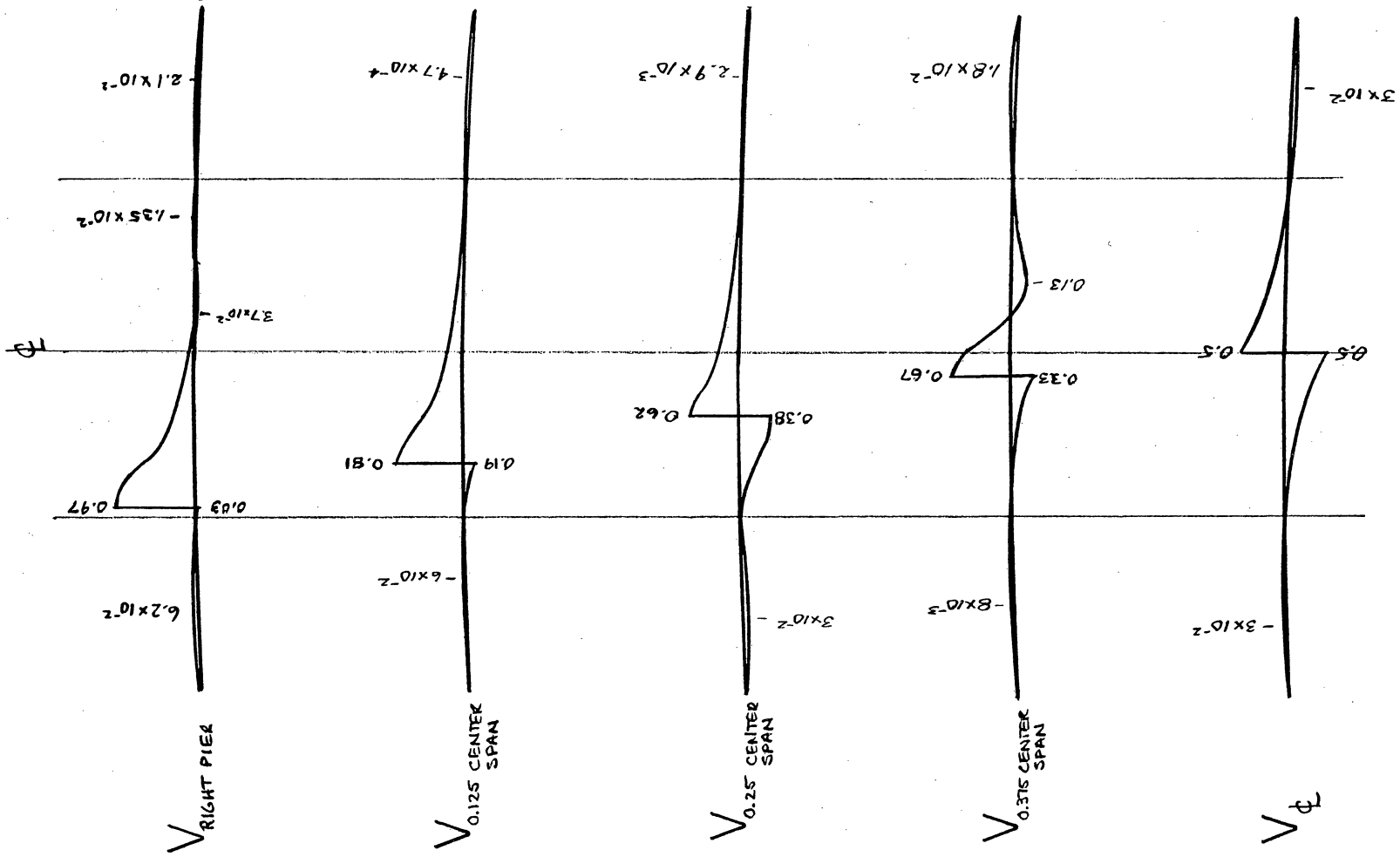


Figure 20. Continued.

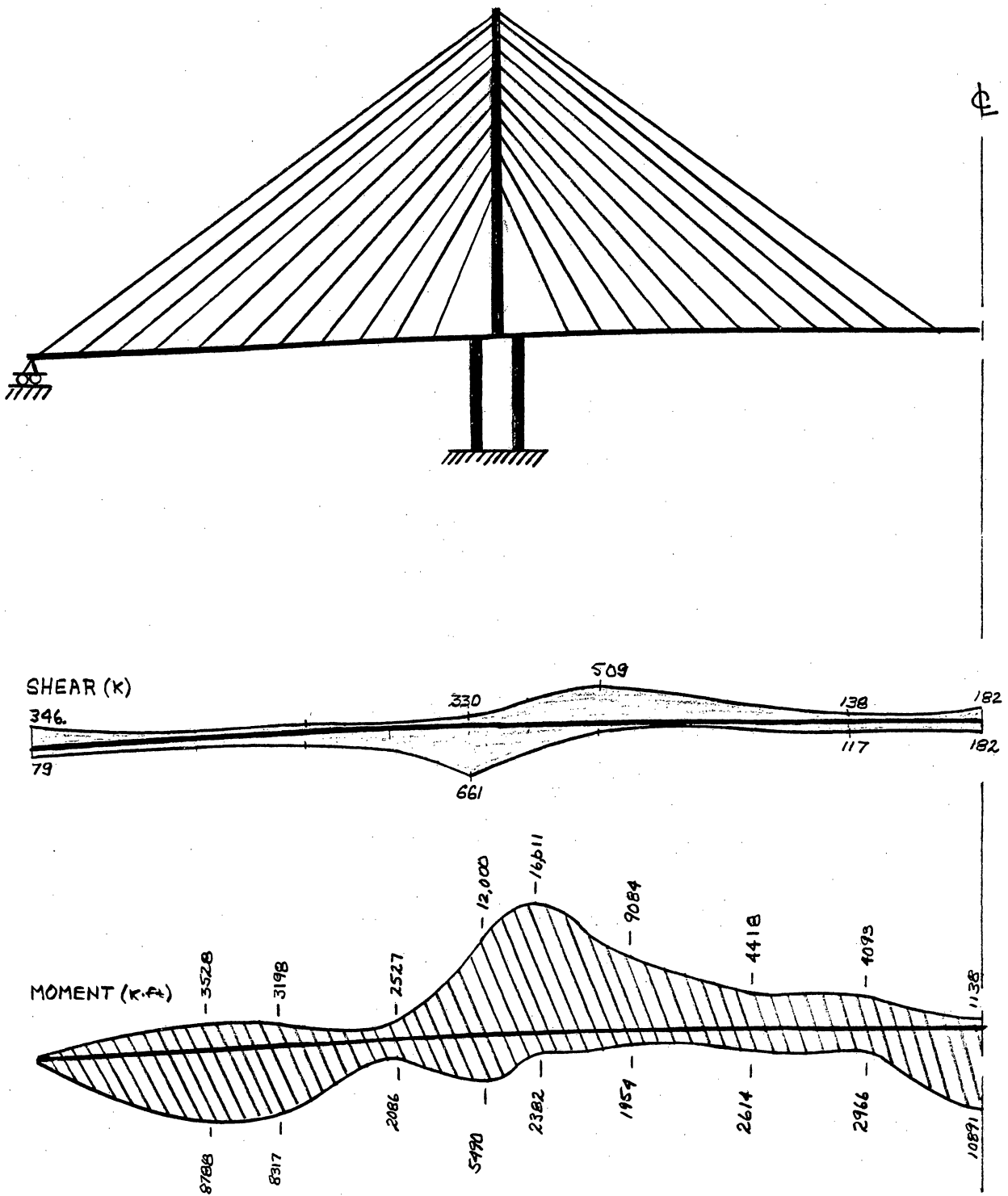


Figure 21. Live load shear and moment envelopes.

3.6 PRESTRESSING DESIGN OF THE GIRDER FOR THE COMPLETED STRUCTURE

The design of the longitudinal prestressing was considered for the completed structure. Although many other loading considerations must be taken into account in a detailed analysis, for the purpose of a preliminary design only the completed span was considered. The design utilized 270 ksi tendons composed of twelve 1/2 inch diameter strands. Using 70 percent of the ultimate force allowed each tendon to be stressed to 347 kips. Prestressing losses were considered in the design. Stresses were checked before and after losses took place to ensure that they were within AASHTO specifications. Likewise, they were checked when the service load moment was applied to the section in question. AASHTO does not permit any tension to exist across any joint between segments during application of service loads. Axial compression in the girder, produced mainly by the horizontal component of the cable stays, was incorporated in the design to alleviate tension stresses as depicted in Equation 3.6 below.

$$f = \pm \frac{P_{Prestress}(e)}{A_{Box}} \pm \frac{M}{S} - \left[\frac{P_{Prestress} + P_{Axial\ force}}{A_{Box}} \right] \quad (3.6)$$

where:

- $P_{Axial\ force}$ = Axial force in girder
- $P_{Prestress}$ = Axial prestress force
- A_{Box} = Area of box girder
- M = Moment
- S = Section modulus, I/c
- f = stress at extreme fiber
- e = Eccentricity of prestressing force

Prestressing losses considered were: shrinkage, elastic shortening, concrete creep, friction, and creep associated with prestressing steel. The procedure outlined in AASHTO was used to calculate these losses (Table 4). The results of the prestressing showed that no tension existed across a joint face and compressive stresses were within limits as required by AASHTO (0.55%)

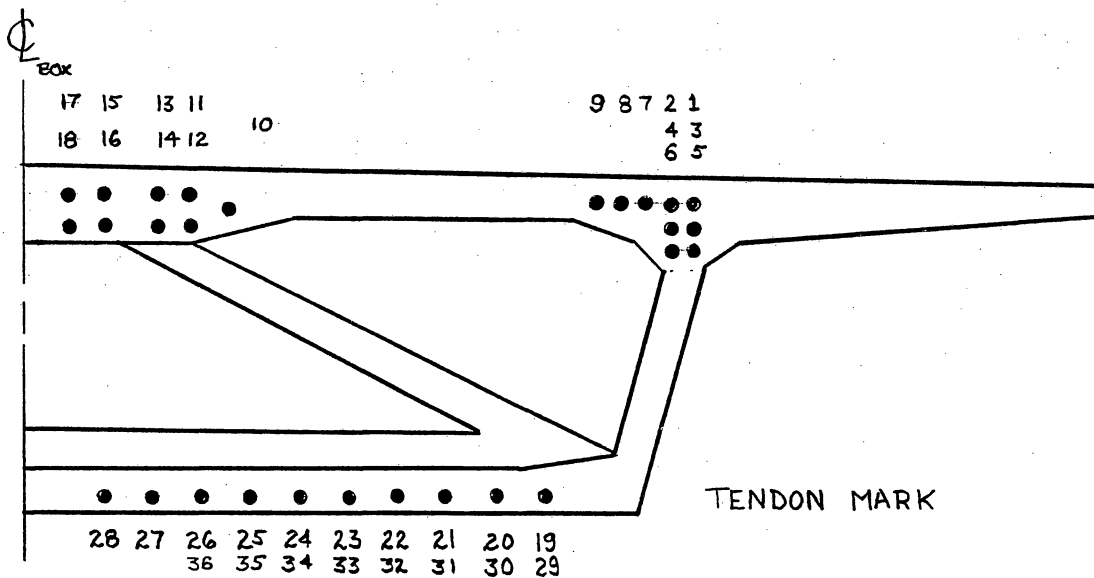
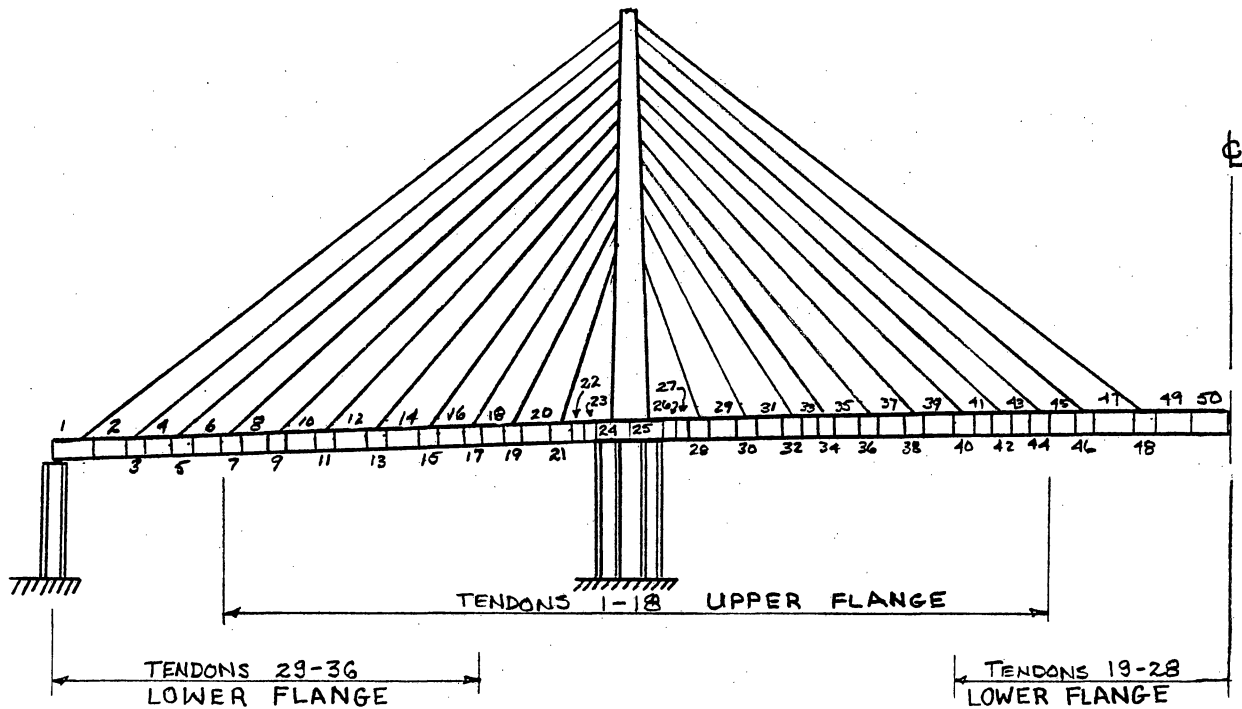


Figure 22. Prestressing tendon reference.

Table 4 : Loss of prestress calculations.

TENDON MARK	LENGTH (ft)	E.S. (psi)	CRC (psi)	FR (psi)	CRS (psi)	f (psi)	f _s (ksi)	ΔT (kips)	T (kips)
1	458	1876.2	2701.4	51,401	5488	62,466	121.5	247.7	446.3
2	435	1876.2	2701.4	49,229	3141	60,947	128.1	223.8	470.2
3	410	1876.2	2701.4	46,867	3849	59,293	129.7	217.7	476.3
4	386	1876.2	2701.4	44,601	4528	57,706	131.3	211.9	482.1
5	359	1876.2	2701.4	42,051	5294	55,922	133.1	205.3	488.7
6	326	1876.2	2701.4	38,934	6229	53,741	135.3	197.3	496.7
7	299	1876.2	2701.4	36,384	6994	51,956	137.0	190.8	503.2
8	274	1876.2	2701.4	34,023	7702	50,303	138.7	184.7	509.3
9	249	1876.2	2701.4	31,661	8411	48,649	140.3	178.6	515.4
10	224	1876.2	2701.4	29,300	9119	46,997	142.0	172.6	521.4
11	200	1876.2	2701.4	27,033	9799	45,410	143.6	166.7	527.3
12	177	1876.2	2701.4	24,861	10,450	43,889	145.1	161.2	532.8
13	144	1876.2	2701.4	21,744	11,386	41,708	147.3	153.2	540.8
14	120	1876.2	2701.4	19,477	12,066	40,121	148.9	147.3	546.7
15	96	1876.2	2701.4	17,210	12,746	38,534	150.5	141.5	552.5
16	71	1876.2	2701.4	14,849	13,454	36,881	152.1	135.4	558.6
17	51	1876.2	2701.4	12,960	14,021	35,558	153.4	130.6	563.4
18	22	1876.2	2701.4	10,221	14,842	33,641	155.4	123.5	570.5
19	248	2238.8	1611.4	31,567	8512	47,129	141.1	176.0	518.0
20	220	2238.8	1611.4	28,922	9305	46,077	142.9	169.2	524.8
21	200	2238.8	1611.4	27,033	9872	44,755	144.2	164.3	529.7
22	200	2238.8	1611.4	24,766	10,552	43,168	145.8	158.5	535.5
23	152	2238.8	1611.4	22,499	11,232	41,581	147.4	152.7	541.3
24	128	2238.8	1611.4	20,233	11,912	39,995	149.0	146.9	547.1
25	100	2238.8	1611.4	17,588	12,706	38,144	150.9	140.1	553.9
26	76	2238.8	1611.4	15,322	13,386	36,558	152.4	134.2	559.8
27	52	2238.8	1611.4	13,055	14,066	34,971	154.0	128.4	565.6
28	28	2238.8	1611.4	10,788	14,745	33,383	155.6	122.6	571.4
29	216	312.6	450.0	28,544	10,421	43,727	145.3	160.6	533.4
30	193	312.6	450.0	26,372	11,073	42,207	146.8	155.0	539.0
31	165	312.6	450.0	23,727	11,866	40,356	148.6	148.2	545.8
32	141	312.6	450.0	21,461	12,547	38,771	150.2	142.4	551.6
33	128	312.6	450.0	20,233	12,915	37,910	151.1	139.2	554.8
34	102	312.6	450.0	17,777	13,652	36,192	152.8	132.9	561.1
35	76	312.6	450.0	15,322	14,388	34,473	154.5	126.6	567.4
36	49	312.6	450.0	12,771	15,154	32,688	156.3	120.0	574.0

SH = Shrinkage = 4000 psi at a relative humidity of 80 percent

Table 5. Stresses due to prestressing and dead load before prestress losses.

SEGMENT NUMBER	AXIAL PRESTRESS (kips)	e (ft)	DEAD LOAD MOMENT (k-ft)	NORMAL FORCE (kips)	TOTAL AXIAL FORCE (kips)	TOTAL MOMENT (k-ft)	f_{Top} (k/ft ²)	f_{Bot} (k/ft ²)
1	684.5	-5.135	-83	0	-3597	685	1.37	-12.47
2	1378.5	-5.283	1311	-1000	-5972	2379	-4.89	-28.16
3	2072.4	-5.135	2706	-1750	-7936	3822	-10.31	-41.23
4	2766.5	-5.283	4875	-1750	-9740	4516	-11.64	-49.59
5	3460.5	-5.332	7044	-2750	-11,410	6210	-18.89	-63.34
6	4154.5	-5.358	8289	-2750	-13,969	6904	-19.16	-73.58
7	5533.2	-4.588	9533	-3550	-15,808	10,471	-37.00	-98.59
8	6921.3	-3.767	10,192	-3550	-15,830	10,471	-36.97	-98.64
9	7614.9	-3.212	10,850	-4250	-13,610	12,559	-52.28	-105.31
10	8308.9	-2.746	10,850	-4250	-11,886	12,559	-54.83	-101.14
11	8308.9	-2.073	10,850	-4950	-6350	13,259	-67.04	-91.78
12	8308.9	-1.527	10,933	-4950	-1756	13,259	-73.83	-80.67
13	8308.9	-0.876	11,016	-5000	3737	13,309	-82.23	-67.67
14	8308.9	-0.035	8276	-5000	7984	13,309	-88.51	-57.40
15	8308.9	0.718	5535	-5450	11,501	13,759	-96.29	-51.49
16	8308.9	1.393	2856	-5450	14,405	13,759	-100.39	-44.46
17	8308.9	2.070	177	-6100	17,377	14,410	-108.73	-41.03
18	8318.5	2.762	-2610	-6100	20,357	14,418	-113.18	-33.86
19	9012.5	2.745	-5396	-6500	19,343	15,512	-117.99	-42.63
20	9706.5	2.999	-7777	-6500	21,340	16,206	-124.94	-41.79
21	10,400.5	3.021	-10,158	-6890	21,262	17,290	-131.07	-48.23
22	11,094.5	2.989	-11,167	-6890	21,994	17,988	-136.17	-50.49
23	11,788.5	3.009	-12,175	-6890	23,201	18,678	-141.90	-51.54
24	PIER SEGMENT (solid section)							
25	PIER SEGMENT (solid section)							
26	12482.48	2.999	-11,500	-6850	25,823	23,982	-176.38	-75.77
27	12482.48	2.982	-10,750	-6850	26,473	19,324	-150.49	-47.35
28	11788.48	3.009	-10,000	-6850	25,472	18,638	-145.06	-45.82
29	11094.48	2.989	-9000	-6500	24,161	17,594	-137.11	-42.97
30	10040.48	3.021	-8000	-6500	23,418	16,900	-132.01	-40.77
31	9706.48	2.999	-7400	-6190	21,718	15,896	-123.71	-39.09
32	9012.48	2.745	-6800	-6190	17,939	15,202	-114.12	-44.23
33	8318.48	2.716	-5500	-5850	17,467	14,168	-107.47	-39.42
34	7624.48	2.711	-4200	-5850	16,475	13,474	-97.75	-45.07
35	6930.48	2.727	-3650	-5200	15,254	12,130	-92.45	-33.22
36	6236.48	2.664	-3100	-5200	13,514	11,436	-85.88	-33.23
37	5542.48	2.584	-2550	-4600	11,772	10,142	-75.85	-29.98
38	4848.48	2.303	-2000	-4600	9168	9448	-68.01	-22.29
39	4154.80	2.303	-1050	-4000	8520	8154	-59.59	-26.39
40	4144.98	1.287	-100	-4000	5238	8155	-54.74	-39.34
41	4144.98	-0.053	700	-3390	480	7534	-44.14	-42.27
42	4144.98	-1.386	1500	-3390	-4244	7534	-37.16	-53.70
43	4144.98	-2.851	3250	-2500	-8563	6645	-25.65	-59.01
44	4144.98	-4.021	4000	-2500	-12,663	6645	-19.59	-68.90
45	4154.48	-5.382	5500	-1800	-16,860	5954	-9.41	-75.10
46	4848.48	-5.389	7000	-1800	-19,128	6648	-10.06	-84.60
47	5542.48	-5.395	9350	-750	-20,550	6292	- 5.91	-85.90
48	6236.48	-5.399	11,700	-750	-21,969	6986	- 7.82	-93.40
49	6930.48	-5.402	15,031	-281	-22,408	7211	- 8.46	-93.70
50	7624.48	-5.405	18,362	-281	-22,848	7905	-11.81	-100.83
51	7634.48	-5.432	18,400	-281	-23,067	7915	-11.54	-101.41

Table 6. Stresses due to prestressing and dead load after prestress losses.

SEGMENT NUMBER	AXIAL PRESTRESS (kips)	e (ft)	DEAD LOAD MOMENT (k-ft)	NORMAL FORCE (kips)	TOTAL MOMENT (k-ft)	TOTAL AXIAL FORCE (kips)	f_{Top} (k/ft ²)	f_{Bot} (k/ft ²)
1	526	-5.135	-83	0	-2618	443	1.31	-8.88
2	1065	-5.283	1311	-1000	-4315	2065	-5.53	-22.34
3	1611	-5.135	2706	-1750	-5566	3361	-11.15	-32.84
4	2162	-5.283	4875	-1750	-6547	3912	-12.88	-38.38
5	2717	-5.332	7044	-2750	-7445	5467	-20.51	-49.52
6	3278	-5.358	8289	-2750	-9272	6028	-21.05	-57.17
7	4283	-4.588	9533	-3550	-10,649	7833	-29.42	-70.91
8	5322	-3.767	10,192	-3550	-11,055	8879	-34.85	-77.92
9	5805	-3.212	10,850	-4250	-9329	10,055	-44.17	-80.52
10	6287	-2.746	10,850	-4250	-11,003	10,537	-44.48	-87.35
11	6200	-2.073	10,850	-4950	-3789	11,150	-58.67	-73.43
12	6131	-1.527	10,933	-4950	-59	11,081	-63.78	-64.02
13	6074	-0.876	11,016	-5000	4261	11,074	-70.13	-53.52
14	6081	-0.035	8276	-5000	2369	11,028	-67.06	-57.84
15	5995	0.718	5535	-5450	5433	11,445	-73.99	-52.83
16	5967	1.393	2856	-5450	10,601	11,417	-81.47	-40.17
17	5956	2.070	177	-6100	12,206	12,056	-87.24	-39.97
18	5962	2.762	-2610	-6100	13,851	12,062	-89.98	-36.02
19	6503	2.745	-5396	-6500	12,454	13,003	-93.35	-44.83
20	7050	2.999	-7777	-6500	13,372	13,550	-97.86	-45.76
21	7602	3.021	-10,158	-6890	12,807	14,492	-102.45	-52.55
22	8160	2.989	-11,167	-6890	13,223	15,050	-106.28	-54.77
23	8724	3.009	-12,175	-6890	14,075	15,614	-110.79	-55.95
24	PIER SEGMENT (solid section)							
25	PIER SEGMENT (solid section)							
26	9294	2.999	-11,500	-6850	16,381	16,144	-117.25	-53.44
27	9294	2.982	-10,750	-6850	16,965	16,144	-118.12	-52.02
28	8724	3.009	-10,000	-6850	16,250	15,574	-113.77	-50.46
29	8160	2.989	-9000	-6500	15,390	14,660	-107.24	-47.28
30	7602	3.021	-8000	-6500	14,966	14,102	-103.39	-45.09
31	7050	2.999	-7400	-6190	13,743	13,240	-96.62	-43.08
32	6503	2.745	-6800	-6190	11,050	12,693	-89.48	-41.57
33	5962	2.716	-5500	-5850	10,961	11,812	-84.27	-41.57
34	5430	2.711	-4200	-5850	10,524	11,280	-80.57	-39.56
35	4902	2.727	-3650	-5200	9721	10,102	-72.59	-34.72
36	4381	2.664	-3100	-5200	8571	9581	-67.88	-34.44
37	3866	2.584	-2550	-4600	7441	8466	-59.79	-30.80
38	3356	2.303	-2000	-4600	5731	7957	-54.33	-31.99
39	2853	2.303	-1050	-4000	5522	6853	-47.66	-26.15
40	2868	1.287	-100	-4000	3284	6868	-44.44	-31.64
41	2904	-0.053	700	-3390	4717	6823	-46.29	-27.92
42	2951	-1.386	1500	-3390	-2009	6401	-33.93	-41.76
43	3071	-2.851	3250	-2500	-5623	5511	-23.46	-45.37
44	3082	-4.021	4000	-2500	-9732	5582	-17.80	-55.71
45	3189	-5.382	5500	-1800	-11664	4989	-11.52	-56.97
46	3743	-5.389	7000	-1800	-13171	5543	-12.49	-63.81
47	4302	-5.395	9350	-750	-13855	5052	-8.65	-62.63
48	4868	-5.399	11,700	-750	-14577	5618	-10.84	-57.64
49	5439	-5.402	15,031	-281	-14350	5720	-11.76	-67.68
50	6005	-5.405	18,362	-281	-14095	6286	-15.41	-70.33
51	6005	-5.432	18,400	-281	-14219	6286	-15.22	-70.62

Table 7. Service load stresses.

SEGMENT NUMBER	MAXIMUM POSITIVE LIVE LOAD MOMENT		MAXIMUM NEGATIVE LIVE LOAD MOMENT			
	(k-ft)	f_{Top} (k/in ²)	f_{Bot} (k/in ²)	(k-ft)	f_{Top} (k/in ²)	f_{Bot} (k/in ²)
1	1250	-0.53	-5.86	-502	-2.81	-10.10
2	2753	-9.60	-15.67	-1105	-3.90	-25.00
3	4250	-17.43	-22.55	-1706	-8.64	-36.95
4	5721	-21.33	-24.54	-2298	-9.49	-43.93
5	6137	-29.58	-34.67	-2464	-16.88	-55.46
6	6935	-31.29	-40.30	-2784	-16.94	-63.89
7	7625	-40.69	-52.46	-3610	-24.91	-78.29
8	8250	-47.04	-57.96	-3312	-29.97	-85.90
9	8776	-57.14	-59.29	-3523	-38.98	-89.02
10	8788	-57.47	-66.09	-3528	-39.28	-95.86
11	8769	-71.62	-52.23	-3520	-53.36	-82.13
12	8765	-76.72	-42.83	-3519	-58.59	-72.52
13	8511	-82.69	-32.96	-3417	-62.58	-65.87
14	8317	-79.34	-37.74	-3198	-62.34	-65.57
15	7250	-84.70	-35.31	-2910	-69.69	-59.87
16	5550	-89.65	-26.77	-2228	-78.17	-45.57
17	3127	-92.13	-32.43	-1255	-89.37	-36.95
18	2200	-93.22	-30.73	-883	-88.67	-38.18
19	2370	-96.84	-39.12	-951	-91.15	-47.15
20	3756	-103.39	-36.71	-2527	-94.11	-51.89
21	4230	-108.68	-42.35	-5684	-94.05	-66.32
22	4987	-113.63	-42.73	-8842	-93.22	-76.16
23	5320	-118.63	-43.12	-12,000	-93.06	-84.98
24	PIER SEGMENT (Solid section)					
25	PIER SEGMENT (solid section)					
26	2382	-120.76	-47.71	-16,325	-93.14	-92.92
27	2295	-121.49	-46.50	-16,611	-93.58	-92.19
28	2056	-116.79	-45.52	-15,938	-90.23	-89.01
29	2028	-110.22	-42.40	-14,000	-86.55	-81.14
30	1997	-106.33	-40.29	-12,756	-84.54	-75.94
31	1954	-99.49	-38.37	-10,987	-80.39	-69.65
32	1937	-92.33	-41.77	-9084	-79.22	-71.56
33	1925	-87.11	-36.94	-8257	-72.01	-61.55
34	1998	-83.51	-34.75	-7985	-68.76	-58.88
35	2257	-75.91	-29.27	-6980	-62.28	-51.60
36	2591	-71.71	-28.24	-5627	-59.53	-48.18
37	2614	-63.64	-24.49	-4418	-53.27	-41.48
38	2687	-58.29	-25.52	-4100	-48.27	-41.92
39	2698	-51.63	-19.63	-4831	-40.52	-37.83
40	2735	-48.47	-25.04	-4890	-37.22	-43.47
41	2870	-50.53	-20.99	-4886	-39.07	-39.73
42	2980	-38.33	-34.55	-4750	-26.92	-53.23
43	3250	-28.61	-37.85	-4228	-17.56	-55.92
44	3787	-13.05	-36.20	-3985	-11.92	-65.33
45	4563	-18.27	-45.92	-3127	-6.91	-64.51
46	4985	-19.86	-51.74	-2987	-8.09	-71.00
47	5273	-16.45	-49.86	-2312	-4.66	-69.15
48	6300	-20.16	-52.39	-1986	-7.93	-72.42
49	7438	-22.76	-49.68	-1200	-10.01	-70.55
50	9127	-28.89	-48.24	-1145	-13.73	-73.07
51	10,891	-28.72	-48.54	-1138	-13.56	-73.34

(Table 5-7). For a concrete strength of 5000 psi this converts to an allowable compression of 2750 psi or 396 ksf.

Table quantity references

Table 4:

Tendon mark refers to Figure 22

Length = the approximate tendon length (ft)

E.S. = the elastic shortening loss (psi)

CRC = the concrete creep loss (psi)

FR = the friction loss (psi)

CRS = the creep of steel loss (psi)

f = the total loss of tendon stress (psi)

f_s = the tendon stress after losses (ksi)

ΔT = the change in tendon force (kips)

T = the resultant axial tendon force (kips)

Table 5 and 6:

Segment number refers to Figure 22

Axial prestress = the tendon force before losses (kips)

e = the resultant tendon eccentricity (ft)

Dead load moment = the total dead load moment (k-ft)

Normal force = the axial force in the girder (kips)

Total moment = D.L. moment + Prestress moment

Axial force = Axial force + Tendon force

f_{Top} = the stress at the extreme top fiber (k/ft^2)

f_{Bot} = the stress at the extreme bottom fiber (k/ft^2)

Table 6 represents the same elements as in Table 5 but after losses have occurred.

Table 7:

Segment number refers to Figure 22

Maximum positive live load moment at segment in question

Maximum negative live load moment at segment in question

f_{Top} = service load stress at the extreme top fiber (k/ft²)

f_{Bot} = service load stress at the extreme bottom fiber (k/ft²)

CHAPTER 4

CONCLUSION

The preceding section outlined a preliminary design of a cable-stayed precast post tensioned box girder bridge. The design was based on a review of theories presented by authors in this advanced field of bridge design. As stated previously, the design only considered the final configuration. Many more models would have to be developed to depict the different stages of construction that would be required to perform a detailed analysis, likewise, separate allowable stress ranges governing construction would have to be considered. Furthermore, a computer analysis program specifically designed to incorporate the different types of elements and stress distribution should be utilized. Shear lag should also be investigated in large box girder sections.

Future trends and developments will greatly influence the cable-stayed bridge. Already, external prestressing inside the closed cell of the box girder is being utilized. This allows top and bottom flanges to be considerably thinner since they do not have to accommodate the post-tensioning ducts. Likewise, this reduces the dead weight of the girder. As these structures become lighter and more flexible, fatigue in the cable-stays may become critical and must be investigated. The application of polymer injected concretes to cable-stayed bridges, will greatly increase the allowable tensile and compressive stress ranges and the use of high strength concretes in the range from 8000 to 10,000 psi have already been shown to be economical (12). The increased stress ranges in the concrete will allow longer spans to be constructed. Likewise, as research continues in the area of cable-stays, designs will become more optimized to exploit their load carrying capacities. In view of these advances, longer and longer spans will be destined to be achieved. As we strive to create longer spans we must not forget the words of F. Strussi, an eminent Swiss engineer (12):

The problem of Long Spans has always fascinated the specialist as well as the laymen. The realization of a bridge with a length of span hitherto unattained not only requires great technical knowledge

and capability, but also intuition and creative courage; it signifies a victory over the forces of nature and progress in battle against human insufficiency.

REFERENCES

1. *AASHTO Standard Specifications for Highway Bridges*, Thirteenth Edition 1983 (as ammended 1984, 1985).
2. *ABAQUS*, Hibbit, Carlson, and Sorrenson, Inc., Version 4.5, 1984
3. *Bethlehem Wire Rope for Bridges, Towers, Aerial Tramways, and Structures*, Bethlehem Steel, Catalog No. 2277-A.
4. Kulka, F. and Thoman, S.J., "Feasibility Study of Standard Sections for Segmental Prestressed Concrete Segmental Bridges," *PCI Journal*, Sept/Oct 1983, pp. 54-77.
5. Lazer, B.E., "Stiffness Analysis of Cable-stayed Bridges," *Journal of the Structural Division*, ASCE, Vol. 98, NO. ST7, Proc. Paper 9036, July, 1972, pp. 1650-1612.
6. Leonhardt, F., *Bridges*, The MIT Press, Cambridge, Mass., 1984
7. Leonhardt, F., Zellner, W., and Svensson, A., "The Columbia River Bridge at Pasco-Kennewick, Washington, USA," *FIP Eighth Congress Proceedings*, May, 1978.
8. Libby, J.R., "Segmental Box Girder Bridge Superstructure Design," *ACI Journal*, May 1976, pp. 279-286.
9. Lin, T.Y., *Design of Prestressed Concrete Structures* , Third Edition, Wiley and Sons, NY, 1981.
10. Mathivat, J., *The Cantilever Construction of Prestressed Concrete Bridges*, Wiley and Sons, NY, 1976.
11. Podolny, W. and Scalzi, J. *Construction and Design of Cable-stayed Bridges* , Wiley and Sons, NY, 1976.
12. Podolny, W. and Muller, J., *Construction and Design of Prestressed Concrete Segmental Bridges*, Wiley and Sons, NY, 1982.
13. Svensson, H., Christopher, B., and Saul, P. "Design of a Cable-stayed Steel Composite Bridge," *Journal of Structural Engineering*, ASCE, Vol.112, No. 3, Mar 1986, pp. 489-504.
14. Tang, M., "Design of Cable-stayed Bridges," *Journal of the Structural Division*, ASCE, Vol. 98, No. ST8, Proc. Paper 1791, Aug., 1972, pp. 1789-1801.

**The vita has been removed from
the scanned document**